ROBUST COMMUNICATION IN A TIME-VARYING NOISY ENVIRONMENT

by

John Michael Wilson

Thesis submitted to the Faculty of the

Virginia Polytechnic Institute and State University

in partial fulfillment of the requirements for the degree of

Master of Science

in

Electrical Engineering

APPROVED:

A. A. (Louis) Beex, Chairman

H. F. VanLandingham

K-B. Yu

November 1987

Blacksburg, Virginia

ROBUST COMMUNICATION IN A TIME-VARYING NOISY ENVIRONMENT

by

John Michael Wilson

A. A. (Louis) Beex, Chairman

Electrical Engineering

(ABSTRACT)

Matched filter detectors are used to detect known signal waveforms transmitted under noisy conditions. Moving-average matched filters (MAMF's) are a class of digital filters whose performance is measured in terms of Signal to Noise Ratio (SNR). The overall performance of a MAMF is described by the SNR Improvement (SNRI) which is the ratio of Output SNR (OSNR) to Input SNR (ISNR). The OSNR and ISNR are the SNR at the output and input of the MAMF respectively. SNRI is maximized by maximizing OSNR since ISNR is fixed for a received signal and noise. The OSNR of a MAMF is a function of the noise autocorrelation sequence and the transmitted signal vector. The maximum OSNR of a MAMF is produced when the signal vector is the eigenvector associated with the smallest eigenvalue of the Toeplitz matrix formed from the noise autocorrelation sequence. If the noise autocorrelation is not known in advance of transmission, or not stationary, then it must be estimated at the receiver. Since autocorrelation estimators derive their estimates from noise samples, i.e. a random process, the estimates are probabilistic. In a practical implementation wherein the signal vector is fixed, the noise is stationary over short periods of time, and the noise autocorrelation sequence is estimated, the SNRI or performance of the MAMF varies and can even become less than unity if either the estimates are poor or the noise characteristics differ from those expected when the signal vectors were selected. A SNRI less than unity is highly undesireable as processing, which is done with the objective of

obtaining higher OSNR than ISNR, i.e. a SNRI greater than unity, has become counterproductive.

This thesis proposes a variation to the classical MAMF communication system and investigates the performance of the resulting MAMF. In the classical MAMF communication system the N-dimensional signal vector is treated as a single vector. In the proposed MAMF communication system, the N-dimensional signal vector is composed of two or more linearly independent basis vectors spanning a signal vector subspace of dimension M. By combining the linearly independent basis vectors in the receiver, one can effectively change the transmitted signal vector to any signal vector in the signal vector subspace to maximize OSNR. The OSNR of a MAMF is a function of the autocorrelation of the noise as well as the signal vector. The autocorrelation of the noise is estimated in both the classical and proposed systems. For relatively few noise samples, the estimated autocorrelation of the noise deviates from the actual autocorrelation. The proposed system is formed from the classical system by preceeding the MAMF with a processor that extracts the received linearly independent basis vectors with additive colored Gaussian noise from the received transmission and combines them to yield maximum OSNR assuming the estimated autocorrelation of the noise is exact. Since the autocorrelation of the noise is estimated from the random noise process, the autocorrelations themselves are probabilistic and hence the maximum OSNR is too. As the estimated noise autocorrelation approaches the actual noise autocorrelation, the OSNR approaches the absolute maximum OSNR for the M-dimensional system. The theoretical aspects of both the classical and proposed MAMF communication systems are developed in this thesis.

The performance of the proposed MAMF communication system is investigated for a practical implementation wherein the signal vector is composed of two linearly independent basis vectors and the noise characteristics vary over time. The performance

of the proposed system is first compared to that of the classical system with both systems using various signal vectors, over various noise colors, and with the exact noise autocorrelation given. The performance comparison between the classical and proposed systems is then repeated with the noise autocorrelation, as in a practical implementation, estimated using either the classical biased or Burg estimator. The performance is measured by SNRI and the results are tabulated and graphed.

Finally, the proposed system is implemented and its performance measured by bit error rates as a function of ISNR. This will show whether SNRI performance is a good prediction of bit error rate performance. The color of the stationary Gaussian noise is kept constant during transmission of a particular bit. The color of the stationary Gaussian noise is changed between bit transmissions to observe the robustness of the system under different colored noise conditions while maintaining the same signal vectors, or signal subspace. The results are again tabulated and graphed.

Acknowledgements

I wish to extend my greatest appreciation to Dr. A. A. Beex, who originated the essential concept for this work, provided guidance during the development, and edited this document; Dr. K-B. Yu and Dr. H. F. VanLandingham who served on my committee; my friends for their moral support; and my parents Glen E. Wilson and Momoko M. Wilson whose love and prayers gave me strength to see this thru.

Table of Contents

List of Illustrations

List of Tables

1.0 INTRODUCTION

All signals transmitted through a channel or medium, such as free space or transmission wires, are subject to additive colored noise. The processing of signals with additive colored noise is thus of considerable interest in communication systems. This thesis investigates a matched filter communication system wherein a matched filter receiving system processes known signals with additive colored noise. The matched filter receiving system is designed and developed to maximize detection and discrimination of the transmitted signals. The element central to the matched filter receiving system is the Moving-Average Matched Filter (MAMF).

The MAMF considered herein is a subset of the class of matched filters. Specifically, the MAMF in the context of this thesis is a class of FIR digital matched filters which performs a weighted sum over finite portions of data at a time, hence MA, and where the filter coefficients are chosen to maximize the probability of detection and discrimination of known signals with additive colored noise, hence MF. There are several reasons for selecting a MAMF. MAMF's can be designed efficiently, they are easy to implement, and are guaranteed to be stable.

The performance of a MAMF system is measured in terms of Signal to Noise Ratio (SNR). SNR is the ratio of signal energy to noise energy. The SNR at the input of the MAMF receiving system shall be referred to as Input SNR (ISNR), and the SNR at the output of the MAMF shall be referred to as Output SNR (OSNR). The improvement to the SNR afforded by the MAMF shall be referred to as SNR Improvement (SNRI) and is the ratio of OSNR to ISNR. In order to design a MAMF, two pieces of information are required: the array of signals that is used to encode the data to be communicated and the autocorrelation of the additive colored noise. For the case where the noise autocorrelation is not known or the noise is not stationary over the entire transmission time, the noise autocorrelation must be estimated. The effect on performance of estimating the noise autocorrelation in classical MAMF receiving systems has been investigated [KAB]. Several other authors have determined a signal vector for a particular noise color which maximizes OSNR of the MAMF system [ADW][JAC][JMK][MBT]. This thesis continues both of these investigations on a variation of the classical MAMF communication system wherein the transmitted signal vector is treated as a single N-dimensional vector while the noise autocorrelation is estimated. The performance of the proposed variation or proposed MAMF communication system is compared to that of the classical MAMF communication system and expressed in terms of SNRI.

The general structure of the classical MAMF communication system is depicted in Figure 1 on page 3. The data to be communicated, $\underline{D}$, is first encoded in the transmitter. Each portion or bit of data is encoded into a fixed N-dimensional signal vector, $\underline{s}_i$. The signal vector is then transmitted through the channel where it is subject to additive colored noise, $\underline{w}$ with a Gaussian distribution. The ISNR of the received signal, $\underline{I}$, which consists of the signal vector with additive colored noise, is measured at the input to the MAMF receiving system. Noise samples, $\underline{w}_2$, are taken from gaps between the

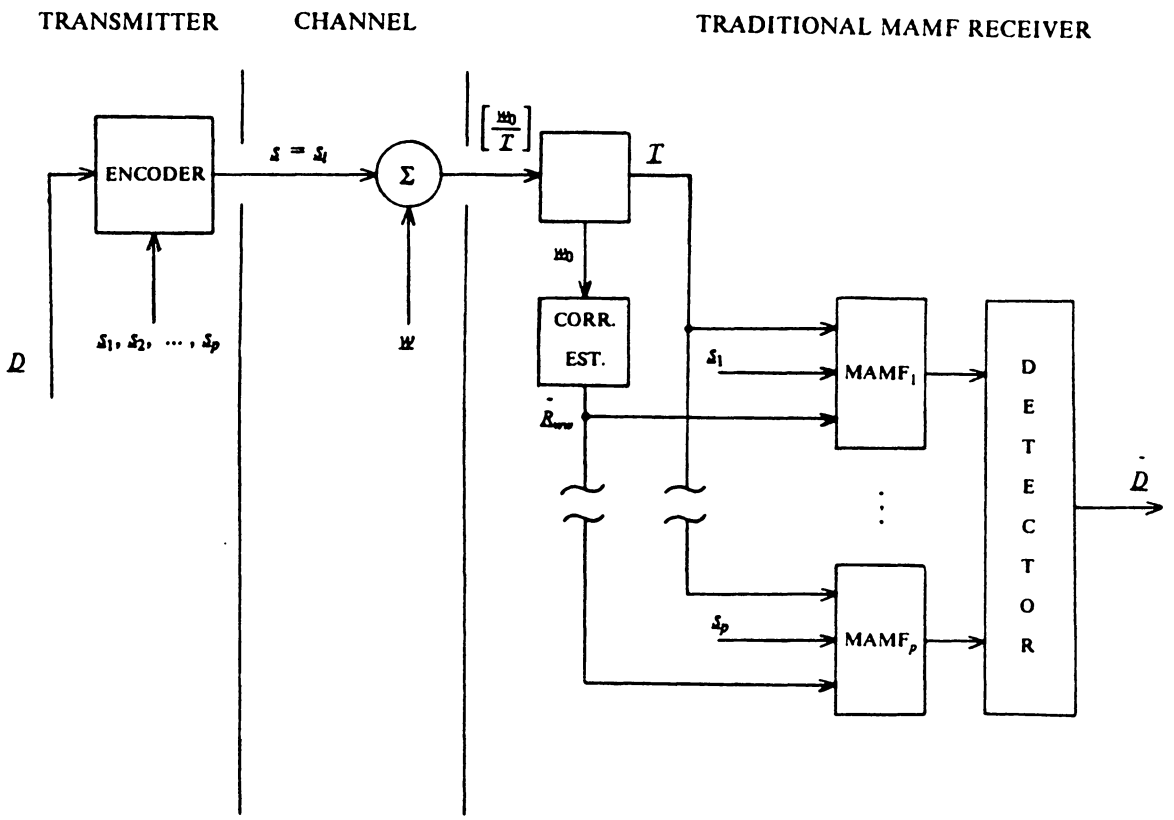

Figure 1. TRADITIONAL MAMF COMMUNICATION SYSTEM

transmitted signal vectors and used to estimate the autocorrelation sequence of the colored noise. The estimated colored noise autocorrelation sequence, $\underline{\hat{R}}_{ww}$, and the set of all signal vectors, $\{\underline{s}_1, \underline{s}_2, \ldots, \underline{s}_K\}$, used to encode the transmitted data are used to form the MAMF(s). The received signal, $\underline{s}_{i1} + \underline{w}_{11}, \underline{s}_{i2} + \underline{w}_{12}, \ldots, \underline{s}_{iK} + \underline{w}_{1K}$, is then processed by either a single MAMF or a bank of MAMF's depending upon the number of signal vectors and the detection scheme. The OSNR is measured at the output of the MAMF(s) and prior to the detector. The detector determines which signal vector was most probably transmitted and hence what data was most probably encoded. The output of the classical MAMF receiving system is the data that was most probably encoded, $\underline{\hat{D}}$. Thus in the classical MAMF communication system, the N-dimensional signal vectors are fixed to represent given sets of data and are not changed to different ones during the entire transmission. One problem which could arise in the aforementioned situation wherein the noise is stationary for only part of the entire transmission is that the fixed signal vectors, if optimized originally to maximize OSNR, will not be optimal if the characteristics of the noise vary. For such cases, it has been and will be shown that the OSNR of a MAMF receiving system could actually be less than the ISNR [KAB], hence a SNRI less than unity. This is highly undesireable since it indicates that the MAMF receiving system degrades the performance of the communication system, rather than improving it.

This thesis investigates an approach wherein the N-dimensional signal vector is composed of a number of M-dimensional linearly independent basis vectors. By combining the linearly independent basis vectors, a high OSNR is attempted to be obtained for a given ISNR. These vectors form a basis for a subspace of an M-dimensional space. By linearly combining the linearly independent basis vectors any vector in the subspace can be created, hence in essence a signal vector subspace is transmitted rather than a single signal vector. Each set of basis vectors, i.e. each signal

vector subspace, is used to represent or encode the data to be transmitted. Upon reception, the linearly independent basis vectors of each signal vector subspace are linearly combined with weighting coefficients to maximize OSNR assuming that the estimated noise autocorrelation is the actual noise autocorrelation. Whether the OSNR is the absolute maximum for the M- dimensional system is dependent upon the accuracy of the noise autocorrelation estimate. The received signal vectors with additive colored Gaussian noise are then combined with the aforementioned weighting coefficients of each signal vector subspace and operated on by the associated matched filter. The basis vectors associated with the filter which has the greatest output signal energy are chosen as the ones most probably transmitted, and hence the data associated with those particular basis vectors is selected.

The general structure of the proposed MAMF communication system is depicted in Figure 2 on page 6. As with the classical MAMF communication system, the data to be communicated, $\underline{D}$, is encoded in the transmitter. Instead of being encoded by a single N-dimensional signal vector, each portion or bit of data is encoded by a set of M-dimensional linearly independent basis vectors - $\{\underline{s}\}_1$, $\{\underline{s}\}_2$, ... , $\{\underline{s}\}_p$. Each of the p sets is composed of K linearly independent basis vectors of length M each. One set, $\{\underline{s}\}_i$, is selected to make up the transmitted signal, $\underline{s}$, and is transmitted through a channel. The transmitted signal is subject to additive colored noise, $\underline{w}$, with a Gaussian distribution. The ISNR of the received signal, $\underline{I}$, which consists of the transmitted signal with additive colored noise, is measured at the input to the MAMF receiving system. Noise samples are taken from a gap between the transmission of each set of linearly independent basis vectors and used to estimate the autocorrelation sequence of the colored noise, $\underline{\hat{R}}_{ww}$. The signal energy at the output of the MAMF is maximized in order to attempt to maximize OSNR. OSNR would indeed be maximized if the estimated autocorrelation were the actual. The OSNR is maximized in this fashion for each set of linearly independent basis

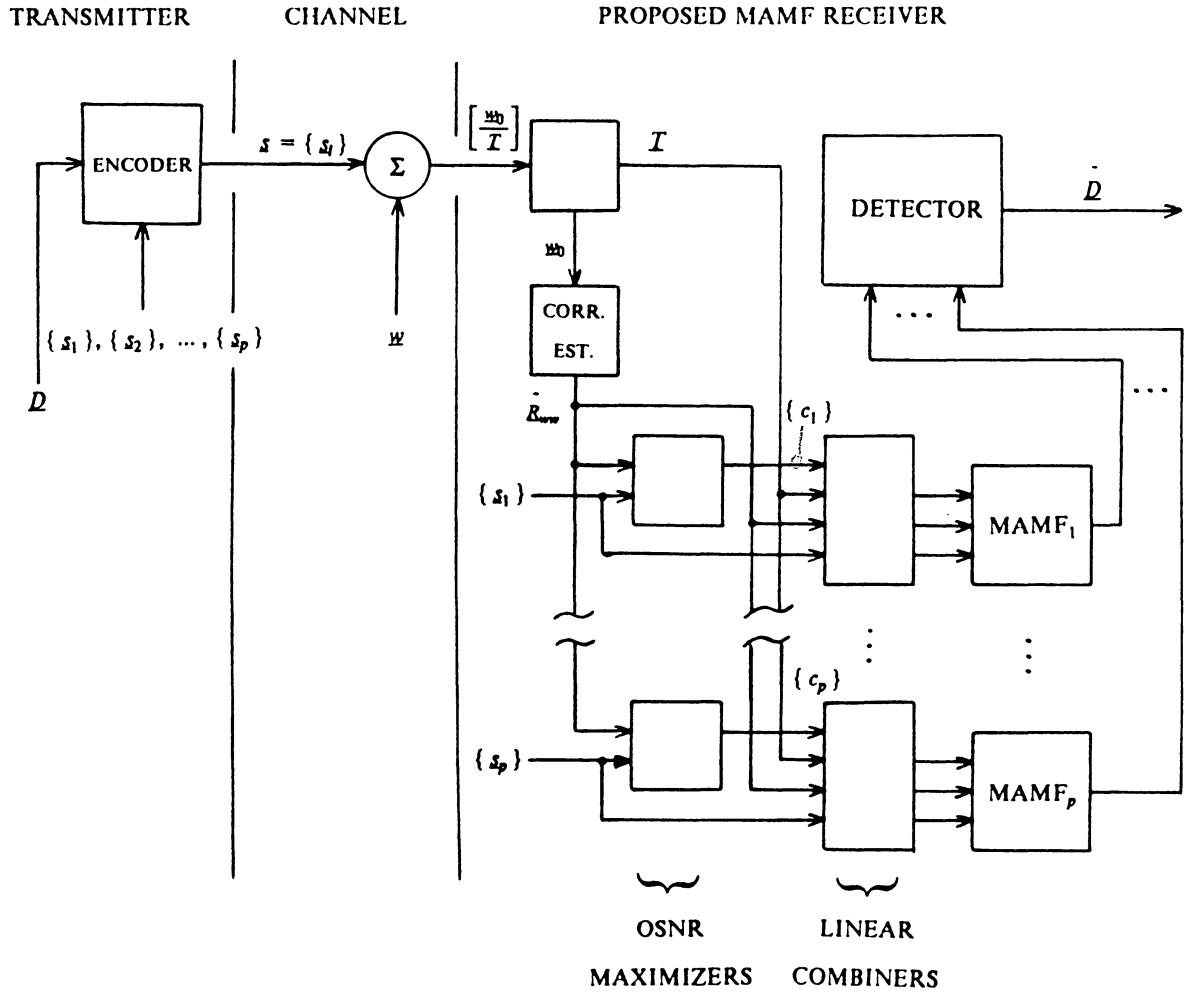

Figure 2. PROPOSED MAMF COMMUNICATION SYSTEM

vectors to determine the coefficients, $\{c_i\}$, used to linearly combine the linearly independent basis vectors. The estimated colored noise autocorrelation sequence, $\underline{\hat{R}}_{ww}$; the sets of linearly independent basis vectors, $\{\underline{s}\}_1$, $\{\underline{s}\}_2$, ... , $\{\underline{s}\}_K$; and the coefficients used to linearly combine the linearly independent basis vectors, $\{c_i\}$, are used to form the MAMF(s). The received signal consisting of the transmitted linearly independent basis vectors with additive colored noise, $\underline{s}_{i1} + \underline{w}_1$, $\underline{s}_{i2} + \underline{w}_2$, ..., $\underline{s}_{iK} + \underline{w}_K$, is then processed by either a single MAMF or a bank of MAMF's depending on the number of sets of basis vectors and the detection scheme. The OSNR is measured at the output of the MAMF(s) and prior to the detector. The detector determines which set of linearly independent basis vectors was most probably transmitted and hence what data was most probably encoded. The output of the proposed MAMF communication system is the data that was most probably encoded, $\underline{\hat{D}}$. Thus in the proposed MAMF communication system the use of a set of M-dimensional signal vectors to encode each portion or bit of data to be transmitted is intended to produce relatively high and/or consistent OSNR greater than ISNR, i.e. SNRI greater than unity.

The theoretical aspects of the classical and proposed MAMF communication systems are developed and summarized in Chapter 2. Correlation estimators, autocorrelation matrices, and the range of the coefficients used to combine the linearly independent basis vectors are discussed and developed in particular. In Chapter 3 several computer analyses are presented which investigate the performance of the classical and proposed MAMF systems under different colored noise conditions with different signal vectors and signal vector subspaces, with the noise autocorrelation either known or estimated. The colored additive noise has a Gaussian distribution. The performance of the classical and proposed MAMF systems is measured in SNRI. The analyses wherein the noise autocorrelation is known provide an upper limit for SNRI, while the analyses wherein the noise autocorrelation is not known yield the SNRI

statistics for a practical implementation. In Chapter 4, the proposed system implementation is simulated on a computer and its performance given in terms of bit error rates as a function of ISNR. All results are tabulated. Conclusions drawn are stated in Chapter 5.

2.0 THEORETICAL DEVELOPMENT

This chapter is concerned with the theoretical development of those portions of the proposed MAMF communication system critical to its design. The chapter begins with a look at the properties of symmetric Toeplitz matrices which play a central role in MAMF design. The properties and choice of correlation estimators are then discussed, followed by investigating the structure and selection of the transmitted signal vector, the structure of the received signal, and the effects of linearly combining the received signal. Finally the general properties and performance of the traditional and proposed MAMF receiver systems are discussed and developed.

2.1 Symmetric Toeplitz Matrices

The symmetric Toeplitz matrices used in a MAMF communication system are formed from the autocorrelation sequence of a colored noise process. The autocorrelation sequence has only real components and so the associated symmetric

Toeplitz matrix, Φ, is real and Hermitian. Note that a symmetric Toeplitz matrix is also doubly symmetric, i.e. it is symmetric about its main and secondary diagonals. Thus the properties of both real Hermitian and doubly symmetric matrices apply to the symmetric Toeplitz matrix formed from the autocorrelation sequence of a colored noise process. Let Φ be an $n \times n$ real symmetric Toeplitz matrix as described above, the properties of Φ which are of particular importance in the context of this thesis are as follows:

1. $\Phi = \overline{\Phi}^T$ (conjugate transpose of Φ) $= \Phi^T$ by definition of real Hermitian matrices.

2. Φ^{-1} is doubly symmetric but not necessarily Toeplitz [JMK].

3. $(\Phi^{-1})^T = \Phi^{-1}$ since Φ^{-1} is doubly symmetric.

4. $\Phi = U \Lambda U^{-1} = U \Lambda U^T$, where U is the modal matrix whose columns contain the eigenvectors of Φ and Λ is the Jordan canonical form of Φ [WLB, p.175].

5. Φ has n orthonormal eigenvectors. To show this one must consider two cases. Either all the eigenvalues of Φ are distinct, or at least one of the eigenvalues is a multiple root of the characteristic equation. If all the eigenvalues of Φ are distinct, then Φ has a full set of n linearly independent eigenvectors. If an eigenvalue of Φ is a multiple root of the characteristic equation, that is it has an algebraic multiplicity greater than one, then Φ is fully degenerate and has a full set of n linearly independent eigenvectors [WLB, p.176]. The full set of n linearly independent eigenvectors can be made orthonormal by the Gram-Schmidt orthogonalization process [WLB, p.102]. Thus Φ has n orthonormal eigenvectors.

6. If Φ has distinct eigenvalues, then it also has $(n + 1)/2$ symmetric and $n/2$ skew symmetric eigenvectors [JMK].

7. If an eigenvalue of Φ has algebraic multiplicity greater than one, then the eigenvectors are not unique and not necessarily symmetric; however, they may be chosen to be symmetric or skew symmetric [JMK].

8. Φ is NND [PAP, p. 179], thus the principal minors and the eigenvalues are greater than or equal to zero [WLB, p.184].

The above properties will be useful in developing the performance of a MAMF receiver and the selection of the transmitted signal vector.

2.2 Correlation Estimators

The work in this thesis is concerned with the practical situation wherein the colored noise is wide-sense stationary for at least the transmission of one signal vector and a short finite period afterwards. For such a situation, the autocorrelation is not known a priori for an entire transmission and must therefore be estimated for each transmitted signal vector. This section first investigates the general properties of two classes of correlation estimators, and then discusses in detail the one selected to be implemented from each class.

2.2.1 Properties

The following definitions describe essential properties for the estimators and their estimates used in this thesis.

A **consistent correlation estimator** produces estimates that approach the actual correlation as the length of the data sequence used to generate the estimates approaches infinity. A matrix Φ is **Non-Negative Definite (NND)** iff $\underline{x}^T \Phi \underline{x} \geq 0$ for all $\underline{x}$. A **(Un)Biased correlation estimator** has an expected value (not) equal to the actual correlation.

The importance of an consistent estimator is that its estimates tend toward the actual correlation for each additional bit of data introduced. The estimated correlation thus has less variance about the actual correlation. The advantage of a consistent estimator is that it gives one control over the variance of the estimates provided one can increase the length of the data sequence used to generate the estimates. The Toeplitz matrix formed from the estimated autocorrelation sequence must be NND. If the Toeplitz correlation matrix is not NND, then the sequence would not necessarily be wide-sense stationary [KAB, p.12] and would thus be a function of time and time origin.; moreover, the eigenvalues and the principal minors of the Toeplitz correlation matrix would not necessarily be greater than or equal to zero, hence computed noise energy and SNRI could be negative, which is physically impossible. Since the correlation estimates are functions of a random process, the estimates themselves are probabilistic and may thus produce estimates that yield a Toeplitz correlation matrix that is not NND [KAB, p.53]. The importance of a biased correlation estimator is that it can bias the estimates so that the Toeplitz correlation matrix is NND.

2.2.2 Moving-Average Estimators

The moving-average estimator generates estimates directly from finite lengths of data samples. The moving-average estimator chosen for the analyses in this thesis is the Classical Biased (CB) estimator. The CB estimator has the smallest standard deviation of the unbiased, diagonal, triangular, exponential and minimum norm moving-average estimators under white, lowpass and bandpass noise as simulated in the work by K.A. Becker [KAB, p.83]. The autocorrelation sequence derived from the CB estimator is given by

$$R_{ww}\text{cb}\,(l) \;=\; \frac{\sum_{i=0}^{N-l-1} w_i\, w_{i+l}}{N} \tag{2.1}$$

where N is the length of the data sequence and $0 \le l \le N-1$. The CB estimator requires relatively few numerical calculations (approx. N log (N)), is consistent, and produces a correlation sequence whose corresponding Toeplitz correlation matrix is NND [KAB, p.17].

2.2.3 Autoregressive Estimators

An autoregressive (AR) estimator is one that models sampled stochastic data as the output of an AR filter with white noise as input. Given a realization or sample sequence from a stochastic process, the AR estimator generates the coefficients for an AR filter, H(z), of order *m*, i.e.

$$H(z) = \frac{G}{A(z)} \tag{2.2}$$

where $A(z) = \sum_{k=0}^{m} a_k z^{-k}$. Once the coefficients, a_k, have been determined, the correlation estimates can be easily generated [DBS].

The AR estimator chosen for the analyses in this thesis is the maximum entropy method (MEM) or Burg estimator. The Burg estimator has a smaller standard deviation than the Itakura AR estimator under white, lowpass and bandpass noise as simulated in the work by K.A. Becker [KAB, p.83]. The Burg estimator is consistent and produces a correlation sequence whose corresponding real symmetric Toeplitz correlation matrix is NND [KAB, pp.28-30].

2.3 *Transmitted and Received Signals*

The MAMF communication system proposed in this thesis is different than the traditional MAMF communication system. The traditional MAMF communication system encodes a bit or specific piece of data with a fixed N-dimensional signal vector as depicted in Figure 1 on page 3. The proposed system encodes each bit or specific piece of data with a fixed N-dimensional signal vector composed of a set of K M-dimensional linearly independent basis vectors as depicted in Figure 2 on page 6. The signal vector for the proposed system is represented as follows:

$$\underline{s} = \left[\underline{s}_1^T \mid \underline{s}_2^T \mid \ \ldots \ \mid \underline{s}_K^T \right] \tag{2.3}$$

The K vectors are linearly independent basis vectors which span a K-dimensional signal vector sub-space of the M-dimensional space, hence in effect a signal vector sub-space is transmitted rather than a single vector. The purpose of transmitting a signal sub-space is that as the noise varies, the signal vector can be changed by linearly combining the basis vectors to produce or maintain a high probability of detection and discrimination of the particular transmitted signal vector.

The signal vector which maximizes the probability of discrimination and detection is an eigenvector of the Toeplitz autocorrelation matrix as will be developed in Section 2.5. It has been determined that the eigenvectors of the Toeplitz autocorrelation matrix, which is also doubly symmetric, are or can be chosen to be either symmetric or antisymmetric [ACB][APB][JMK]. This facilitates the selection of linearly independent basis vectors by selecting only those that are symmetric or antisymmetric. Up to this point, the only restriction placed upon the basis vectors is that they be linearly independent in each set. The purpose of the MAMF receiver is to distinguish as well as detect one transmitted signal vector from another or in this case one set of basis vectors from another. If the signal vector sub-spaces were not parallel to one another, then there would exist an infinite number of vectors along the intersection of the sub-spaces that could not be distinguished. Thus the existence of an infinite number of vectors belonging to at least two different sub-spaces makes the task of determining to which sub-space the signal vectors belongs to impossible and hence the chance for error is increased. If the basis vectors of each set of basis vectors is orthogonal to the basis vectors of all the other sets of basis vectors, then the sub-spaces associated with each set would be parallel and there would exist no vectors belonging to more than one sub-space and hence the increased chance for error would be eliminated. The number and length of the orthornormal basis vectors making up the transmitted signal vector is dependent upon the number of different pieces of information to be encoded. For each piece of

information, $K \geq 2$ linearly independent basis vectors are required so that a minimal sub-space of dimension 2 is spanned. Given p different pieces of information, the minimum length of each basis vector is $K \times p$ to insure p parallel sub-spaces. The linearly independent basis vectors should thus be chosen either symmetric or antisymmetric, normal to the basis vectors of all other sets of basis vectors, and their number and length dependent upon the number of bits or pieces of information to be encoded.

The colored noise shall be assumed stationary over at least one transmission of a set of one N-dimensional signal vector, hence the colored noise characteristics must be estimated for each N-dimensional signal vector. Samples of the colored noise are required to estimate its characteristics, thus each transmission of a N-dimensional signal vector shall be preceeded by a gap wherein no signal information is transmitted. The information content of the gap will consist of the colored channel noise. The colored noise vector used to estimate the colored noise autocorrelation sequence shall be composed of samples taken from the gap between the transmission of each N-dimensional signal vector.

From Figure 1 on page 3 and Figure 2 on page 6, the transmitted signal vector is subject to additive colored noise in the channel so that the received signal vector, $\underline{I}$, is composed of the transmitted signal vector, $\underline{s}$, and the additive colored noise, $\underline{w}$. The received transmission thus consists of the colored noise vector, $\underline{w}_0$ followed by the received signal vector, $\underline{I}$. The received transmissions for the traditional and proposed communication systems are represented as follows:

$$\text{Traditional: } \left[\underline{w}_0^T \mid \underline{I}^T \right] = \left[\underline{w}^T \mid (\underline{s} + \underline{w})^T \right] \tag{2.4a}$$

$$\text{Proposed: } \left[\underline{w}_0^T \mid \underline{I}^T \right] = \left[\underline{w}_0^T \mid (\underline{s}_1 + \underline{w}_1)^T \mid (\underline{s}_i + \underline{w}_i)^T \mid \ldots \mid (\underline{s}_K + \underline{w}_K)^T \right] \tag{2.4b}$$

where the colored noise vector, $\underline{w}_i$, is the noise associated with *i-th* basis vector, and the second order characteristics are assumed to be the same for $i \in [0,K]$. The noise is thus assumed wide-sense stationary for each received transmission as given in equations (2.4a) and (2.4b).

2.4 Linear Combination

The principal feature of the proposed MAMF communication system that differentiates it from the traditional MAMF communication system is that the transmitted signal vector is composed of K M-dimensional linearly independent basis vectors instead of a single N-dimensional signal vector. By linearly combining the K linearly independent basis vectors, any vector in the sub-space **K** can be formed. Thus instead of transmitting a single vector in a N-dimensional space as in the traditional MAMF communication system, a K-dimensional signal vector sub-space of an M-dimensional space is effectively transmitted. From equation (2.4b) note that not only are the linearly independent basis vectors, $\underline{s}_i$, of the received signal being linearly combined, but so are their associated additive noise vectors, $\underline{w}_i$. The restrictions and effects of linearly combining the received signal and noise vectors are investigated in the following sections.

2.4.1 Linearly Independent Basis Vectors

The linearly independent basis vectors, $\underline{s}_1$, $\underline{s}_2$, ... , $\underline{s}_i$, ... , and $\underline{s}_K$ are combined lineary to achieve any vector in the sub-space **K**. The linear combination of linearly independent basis vectors is written as follows:

$$\begin{aligned} \underline{\tilde{s}} &= \left[\underline{s}_1 \mid \underline{s}_2 \mid \cdots \mid \underline{s}_K \right] \begin{bmatrix} c_1 \\ c_2 \\ \vdots \\ c_K \end{bmatrix} \\ &= c_1 \underline{s}_1 + c_2 \underline{s}_2 + \cdots + c_i \underline{s}_i + \cdots + c_K \underline{s}_K \end{aligned} \tag{2.5}$$

where the c_i's are real coefficients and the $\underline{s}_i$'s are linearly independent of each other. The only restrictions on the coefficients is that one is dependent while the remaining $K - 1$ are independent. The task of maximizing signal energy out of the MAMF becomes quite formidable if there exist no restrictions on the ranges of the coefficients. The coefficients are thus restricted so that the energy of the linearly combined signal vector, $E_{\tilde{s}}$, is equal to the energy of the transmitted signal vector, E_s:

$$
\begin{aligned}
E_{\tilde{s}} &= <\tilde{\underline{s}}, \tilde{\underline{s}}> \\
&= \sum_{l=1}^{K} \sum_{j=1}^{K} c_l c_j \underline{s}_l^T \underline{s}_j \\
&= \sum_{i=1}^{K} c_l^2 < \underline{s}_l, \underline{s}_l > + \sum_{\substack{l,j=1 \\ l \neq j}}^{K} c_l c_j < \underline{s}_l, \underline{s}_j > \\
&= E_s \\
&= <\underline{s}, \underline{s}> \\
&= \sum_{l=1}^{K} \sum_{j=1}^{K} \underline{s}_l^T \underline{s}_j \\
&= \sum_{l=1}^{K} < \underline{s}_l, \underline{s}_i > + \sum_{\substack{l,j=1 \\ l \neq j}}^{K} < \underline{s}_i, \underline{s}_j >
\end{aligned}
\tag{2.6}
$$

Thus the coefficients used to linearly combine the linearly independent basis vectors and their associated noise vectors are constrained by

$$
\sum_{i=1}^{K} c_l^2 < \underline{s}_l, \underline{s}_l > + \sum_{\substack{l,j=1 \\ l \neq j}}^{K} c_l c_j < \underline{s}_l, \underline{s}_j > \quad = \quad \sum_{i=1}^{K} < \underline{s}_i, \underline{s}_l > + \sum_{\substack{i,j=1 \\ i \neq j}}^{K} < \underline{s}_l, \underline{s}_j > \tag{2.7}
$$

Equation (2.7) is simplified if the linearly independent basis vectors are chosen such that each basis vector within a particular set is orthonormal to the others, i.e.

$$
\begin{aligned}
< \underline{s}_l, \underline{s}_j > &= 0 \text{ for } i \neq j \text{ and} \\
&= 1 \text{ for } i = j
\end{aligned}
\tag{2.8}
$$

The energy of the transmitted signal vector simplifies to

$$
\begin{aligned}
E_s &= \sum_{l=1}^{K} < \underline{s}_l, \underline{s}_l > + \sum_{\substack{i,j=1 \\ l \neq j}}^{K} < \underline{s}_i, \underline{s}_j > \\
&= K
\end{aligned}
\tag{2.9}
$$

where K is the number of basis vectors in the N- dimensional transmitted signal vector. The energy of the linearly combined signal vector simplifies to

$$\begin{aligned} E_s &= \sum_{i=1}^{K} c_i^2 < \underline{s}_i, \underline{s}_i > + \sum_{\substack{i,j=1 \\ i \neq j}}^{K} c_i c_j < \underline{s}_i, \underline{s}_j > \\ &= \sum_{i=1}^{K} c_i^2 \end{aligned} \tag{2.10}$$

Thus the constraint expressed in equation (2.7) simplifies to

$$\sum_{i=1}^{K} c_i^2 = E_s = K \tag{2.11}$$

where K is the number of orthonormal basis vectors in the N-dimensional signal vector.

2.4.2 Additive Colored Noise

Linearly combining the received set of K signal vectors combines not only the linearly independent basis vectors, but also the additive colored noise vector associated with each one. The colored noise after linearly combining the $\underline{w}_i$'s, represented by $\underline{w}_v$, is defined as

$$\underline{w}_v = \sum_{i=1}^{K} c_i \underline{w}_i \tag{2.12}$$

Before developing the autocorrelation for the resulting noise, $\underline{w}_v$, some relationships essential to the development are introduced first.

1. Since the noise is assumed stationary over the duration of the noise vector plus the K vectors forming the received signal vector, the autocorrelation sequence of the *i-th* noise vector, $\underline{w}_i$, is equal to the autocorrelation sequence of the noise process $\underline{w}$, i.e.

$$E\left[\underline{w}_i(n+l)\,\underline{w}_i(n)\right] = R_{ww}(l) \text{ for } 0 \le i \le K \tag{2.13}$$

2. Since the transmitted signal vector is composed of concatenated linearly independent basis vectors,

$$\begin{aligned} \underline{w}_i(n)\,\underline{w}_j(n) &= \underline{w}_i(n)\;\underline{w}_i(n+(j-i)M) \\ &= \underline{w}_i(n+(i-j)M)\;\underline{w}_j(n) \end{aligned} \tag{2.14}$$

where M is the length of a basis vector.

3. From the property of reflection invariance

$$R_{xx}(k) = R_{xx}(-k) \tag{2.15}$$

where $R_{xx}(k)$ is the autocorrelation sequence of x at lag k.

The autocorrelation sequence for $\underline{w}_v$, $R_v(l)$, is developed as follows:

$$\begin{aligned} R_v(l) &= \mathrm{E}\left[\underline{w}_v(n+l)\,\underline{w}_v(n)\right] \\ &= \mathrm{E}\left[\sum_{i=1}^{K} c_i\,\underline{w}_i(n+l)\sum_{j=1}^{K} c_j\,\underline{w}_j(n)\right] \\ &= \sum_{i=1}^{K}\sum_{j=1}^{K} c_i\,c_j\,\mathrm{E}\left[\underline{w}_i(n+l)\;\underline{w}_j(n)\right] \\ &= \sum_{i=1}^{K}\sum_{j=1}^{K} c_i\,c_j\,\mathrm{E}\left[\underline{w}_j(n+l+(i-j)M)\;\underline{w}_j(n)\right] \\ &= \sum_{i=1}^{K}\sum_{j=1}^{K} c_i\,c_j\,R_{ww}(l+(i-j)M) \\ &= \sum_{i=1}^{K}\sum_{j=1}^{K} c_i\,c_j\,R_{ww}((j-i)M-l) \end{aligned} \tag{2.16}$$

The summation over j can be split into three cases as follows:

$$\begin{aligned} R_v(l) &= \sum_{i=1}^{K}\sum_{j=1}^{K} c_i\,c_j\,R_{ww}((j-i)M-l) \\ &\quad \sum_{j<i} \\ &\quad + \sum_{i=1}^{K} c_i^2\,R_{ww}(l) \\ &\quad + \sum_{l=1}^{K}\sum_{j=1}^{K} c_i\,c_j\,R_{ww}((j-i)M-l) \\ &\quad\quad j>i \end{aligned} \tag{2.17}$$

Interchanging i and j in the first term and using the property of reflection invariance expressed in equation (2.15) on the first term of equation (2.17) yields

$$\begin{aligned} R_v(l) &= \sum_{i=1}^{K}\sum_{j=1}^{K} c_i\,c_j\,R_{ww}((j-i)M+l) \\ &\quad \sum_{j>i} \\ &\quad + \sum_{i=1}^{K} c_i^2\,R_{ww}(l) \\ &\quad + \sum_{l=1}^{K}\sum_{j=1}^{K} c_i\,c_j\,R_{ww}((j-i)M-l) \\ &\quad\quad j>l \end{aligned} \tag{2.18}$$

The summations of the first and last terms may be combined and rewritten as follows:

$$\begin{aligned} R_v(l) &= \sum_{i=1}^{K} c_i^2 R_{ww}(l) \\ &\quad + \sum_{i=1}^{K-1} \sum_{j=i+1}^{K} c_i c_j \left[R_{ww}((j-i)M + l) + R_{ww}((j-i)M - l) \right] \end{aligned} \tag{2.19}$$

Thus the effects of linearly combining the colored noise produces a linear relationship between $R_v(l)$ and $R_{ww}(l)$. Note however that the relationships between the colored noise sequences $\underline{w}_i$ and $\underline{w}_v$ and their associated autocorrelation sequences $R_{ww}(l)$ and $R_v(l)$ respectively are highly non-linear.

2.5 *Moving Average Matched Filter*

The element central to the MAMF receiver or detector and the MAMF communication system is the MAMF itself. Block diagrams of the traditional and proposed MAMF receivers are provided in Figure 3 on page 24 and Figure 4 on page 25 respectively. The role of a MAMF is to maximize OSNR with respect to a given ISNR at some particular time n_0. Note that ISNR, OSNR and SNRI are all functions of the signal and noise vectors which are functions of time, thus ISNR, OSNR and SNRI are functions of time. OSNR and SNRI shall henceforth be defined at the time n_0 unless specified otherwise. The time, n_0, shall be equal to N-1, where N is the length of the impulse response of the MAMF. ISNR shall be defined at the time prior to n_0 when $\underline{I}$ was received which brings about the associated OSNR and hence SNRI. Creating an OSNR greater than the ISNR, i.e. a SNRI greater than unity, improves the probability of detection and discrimination of a known signal in additive colored noise.

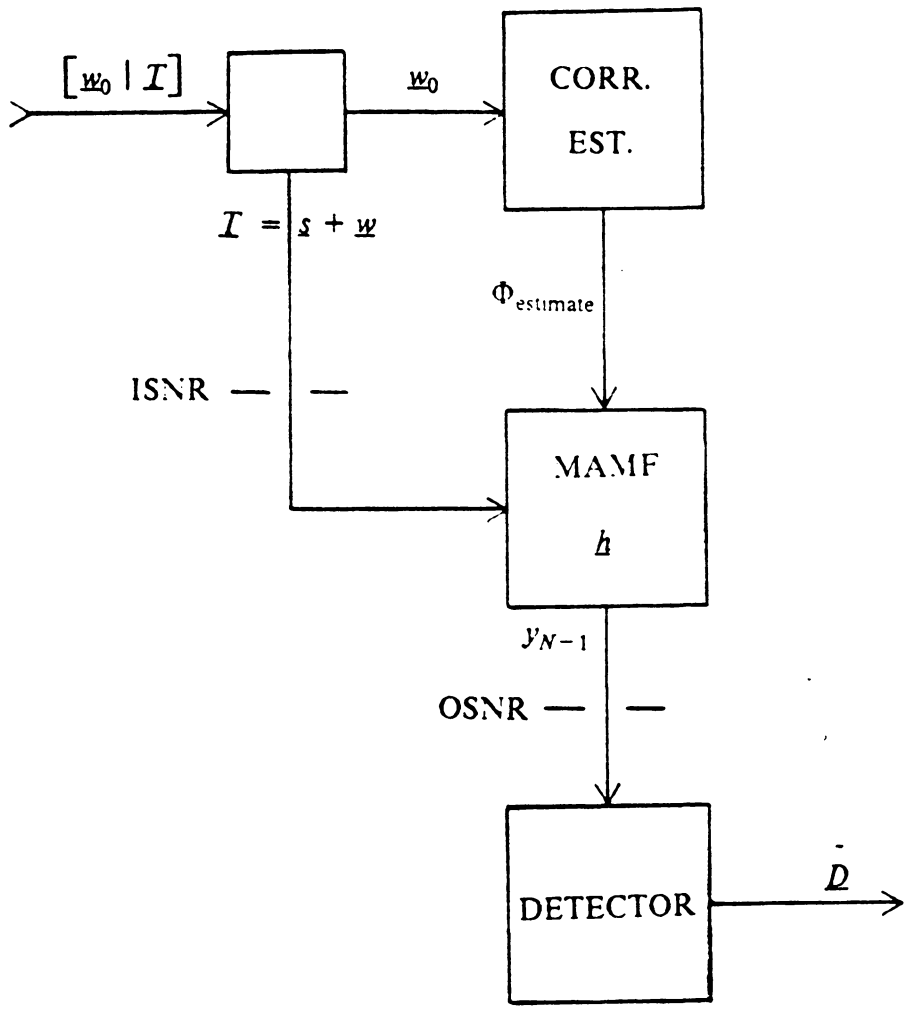

Figure 3. TRADITIONAL MAMF RECEIVER BLOCK DIAGRAM

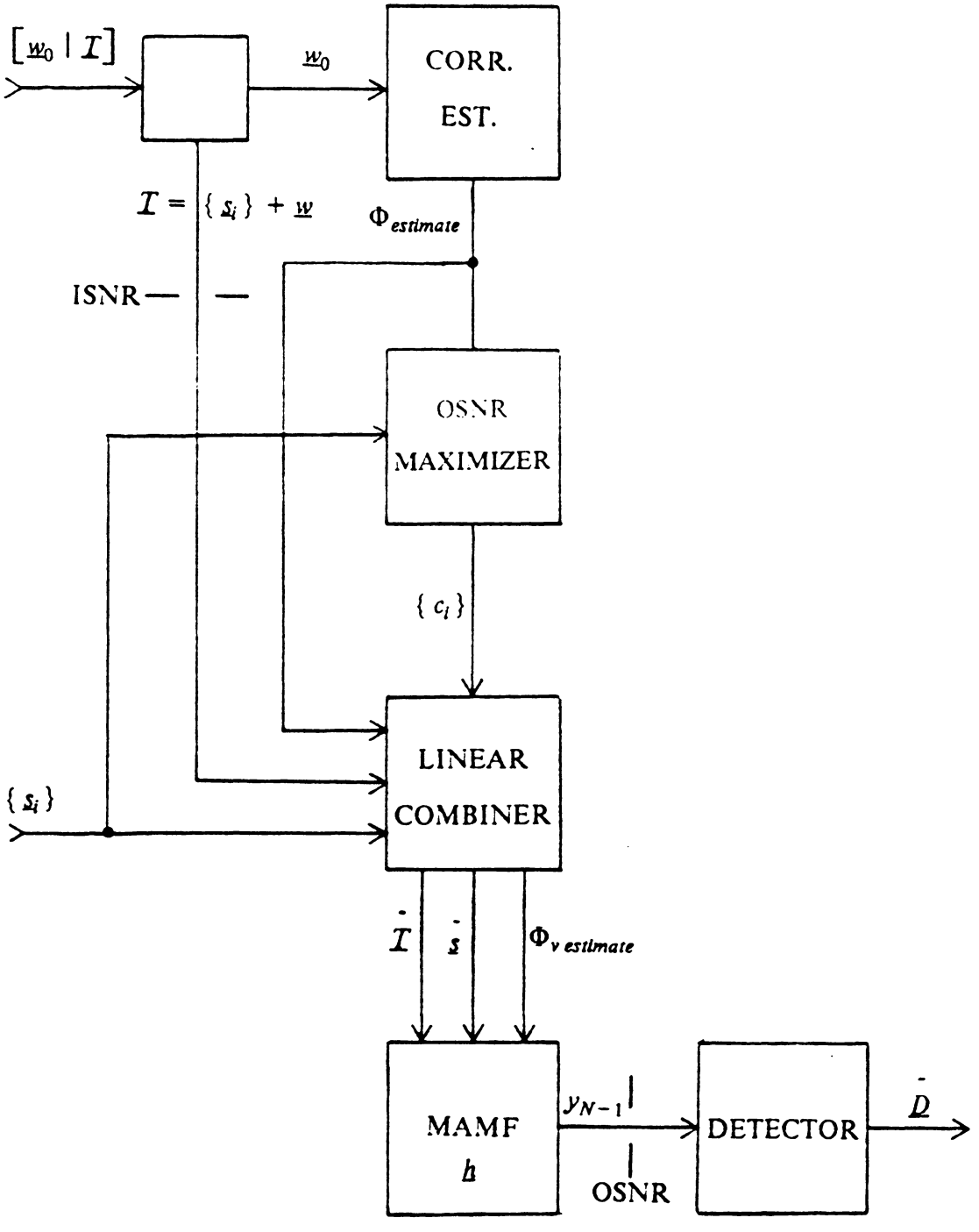

Figure 4. PROPOSED MAMF RECEIVER BLOCK DIAGRAM

By doing so, the MAMF improves the performance of the receiver and hence the communication system. However, if the SNRI is less than unity, the MAMF degrades the performance of the receiver and the communication system.

2.5.1 Characteristics

From Figure 3 on page 24, $\underline{T}$ is the received signal which is corrupted by the additive colored noise and $\underline{h}$ is the impulse response of the filter. The output of the MAMF at time N-1 is

$$\begin{aligned} y_{N-1} &= \sum_{l=0}^{N-1} t_{N-1-l}\, h_l \\ &= \underline{T}^T \underline{h} \end{aligned} \tag{2.20}$$

where

$$\begin{aligned} \underline{T} &= [\, t_{N-1} \;\; t_{N-2} \;\; \cdots \;\; t_0 \,]^T \\ &= [\, s_{N-1}+w_{N-1} \;\; s_{N-2}+w_{N-2} \;\; \cdots \;\; s_0+w_0 \,]^T \\ &= \underline{s} + \underline{w} \end{aligned} \tag{2.21}$$

and

$$\underline{h} = [\, h_0 \;\; h_1 \;\; \cdots \;\; h_{N-1} \,]^T \tag{2.22}$$

Since the filter is of finite length, N, and so operates on a finite portion of the input alone, the filter is a stable FIR filter. As will be shown later, the design of a MAMF requires the signal vector and the autocorrelation of the noise. With the Levinson algorithm, a MAMF can be designed efficiently once the necessary information is given and/or determined. The structure of a MAMF as depicted in Figure 5 on page 28 is a

series of multiply and add sections. Such as structure is easy to implement in software and hardware - including custom and semi-custom VLSI. Thus a MAMF is guaranteed to be stable, can be designed efficiently, and is easy to implement.

2.5.2 Performance

As previously mentioned, the performance of a MAMF receiver is measured by its SNRI which is the ratio of OSNR to ISNR. From Figure 3 on page 24 and Figure 4 on page 25, ISNR is measured at the input of the MAMF receiver and is the ratio of the signal energy to the noise energy in the received transmission, $\underline{T}$. The energy in the received transmission, E_T, is given by

$$E_T = <\underline{T}, \underline{T}> \tag{2.23}$$

where $\underline{T} = \underline{s} + \underline{w}$ as depicted in Figure 3 on page 24 and equations (2.4a) and (2.4b).

Since the colored noise, $\underline{w}$, is additive, superposition can be used to derive ISNR. The signal energy at the input of the MAMF receiver, E_s *input*, is equal to the energy at the input of the MAMF when no noise is present, and is given by

$$\begin{aligned} E_s \, input &= <\underline{s}, \underline{s}> \\ &= \underline{s}^T \underline{s} \end{aligned} \tag{2.24}$$

The noise energy at the input of the MAMF receiver, E_w *input*, is equal to the energy at the input of the MAMF when no signal is present. Since the colored noise is a wide-sense stationary stochastic process, E_w *input*, is equal to its autocorrelation at zero lag and is given by

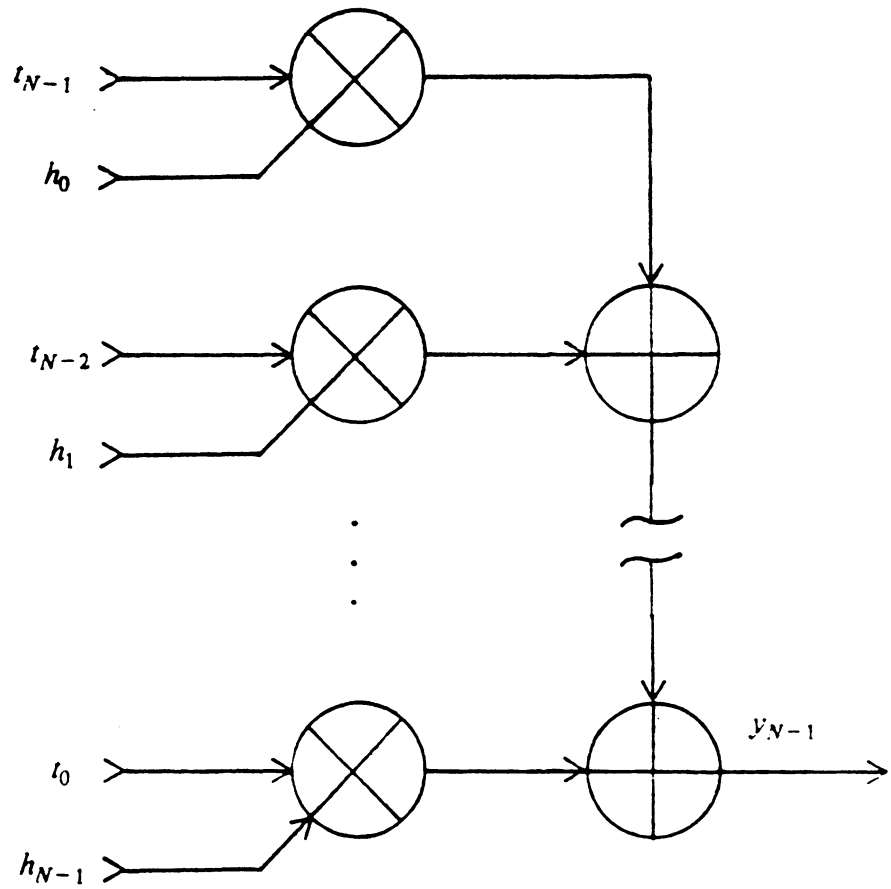

Figure 5. MAMF STRUCTURE

$$
\begin{aligned}
E_w\ input &= \mathrm{E}\left[\, w_i^2 \,\right] \text{ for } -\infty \le i \le \infty \\
&= R_{ww}(0)
\end{aligned}
\tag{2.25}
$$

where $\mathrm{E}[\, w_i^2 \,]$ is the mean of w_i^2 and $R_{ww}(l)$ is the autocorrelation of w_i at lag l. Hence from equations (2.24) and (2.25) and the definition of ISNR,

$$
ISNR = \frac{\underline{s}^T \underline{s}}{R_{ww}(0)} \tag{2.26}
$$

By the principle of superposition, the signal energy at the output of the MAMF, $E_s\ output$, at time N-1 is equal to the energy at the output of the MAMF when no noise is present. From equation (2.20), $E_s\ output$ is given by

$$
\begin{aligned}
E_s\ output &= y_{N-1}^2 \\
&= \left(\sum_{l=0}^{N-1} s_{N-1-l}\, h_l \right)^2 \\
&= \left(\underline{s}^T \underline{h} \right)^2
\end{aligned}
\tag{2.27}
$$

The noise energy at the output of the MAMF, $E_w\ output$, at time N-1 is equal to the energy at the output of the MAMF when no signal is present and is given by

$$
\begin{aligned}
E_w\ output &= \mathrm{E}\left[\, y_{N-1}^2 \,\right] \\
&= \mathrm{E}\left[\left(\sum_{l=0}^{N-1} w_{N-1-l}\, h_i \right)^2 \right] \\
&= \mathrm{E}\left[\sum_{l=0}^{N-1} \sum_{j=0}^{N-1} h_l\, w_{N-1-l}\, h_j\, w_{N-1-j} \right] \\
&= \sum_{l=0}^{N-1} \sum_{j=0}^{N-1} h_l\, h_j\, \mathrm{E}\left[\, w_{N-1-l}\, w_{N-1-j} \,\right] \\
&= \sum_{l=0}^{N-1} \sum_{j=0}^{N-1} h_i\, h_j\, \varphi_{l-j} \\
&= \underline{h}^T \Phi\, \underline{h}
\end{aligned}
\tag{2.28}
$$

where φ_k are the autocorrelations of the colored noise at lag k and Φ is the NxN real symmetric Toeplitz matrix formed from the colored noise autocorrelation sequence with first row $[\,\varphi_0\,\varphi_1\,\cdots\,\varphi_{N-1}\,]$.

Hence from equations (2.27) and (2.28) and the definition of OSNR,

$$OSNR = \frac{(\underline{s}^T \underline{h})^2}{\underline{h}^T \Phi \underline{h}} \tag{2.29}$$

The general performance of a MAMF receiver is thus described by ISNR, equation (2.26); OSNR, equation (2.29); and SNRI, the ratio of OSNR to ISNR.

2.5.3 Optimal Performance

For a given signal vector energy and colored noise, ISNR is fixed, and so maximizing OSNR maximizes SNRI. OSNR is maximized using the Lagrangian multiplier technique where E_w *output* is constrained to be equal to an arbitrary constant K and the root of E_s *input* is maximized. The Lagrangian equation is

$$J(\underline{h}) = \underline{s}^T \underline{h} + \lambda \left(K - \underline{h}^T \Phi \underline{h} \right) \tag{2.30}$$

where λ is a Lagrangian multiplier.

Taking the partial derivative of equation (2.30) with respect to $\underline{h}$ and setting the result equal to zero yields

$$\frac{\partial J(\underline{h})}{\partial \underline{h}} = \underline{s} - 2\lambda \Phi \underline{h} = \underline{0} \tag{2.31}$$

Providing Φ is not singular, solving for $\underline{h}$ produces

$$\underline{h} = \frac{\Phi^{-1}\underline{s}}{2\lambda} \tag{2.32}$$

Note that multiplying $\underline{h}$ by an arbitrary constant, c, does not change OSNR.

$$\begin{aligned} \frac{(\underline{s}^T c\,\underline{h})^2}{c\,\underline{h}^T \Phi\, c\,\underline{h}} &= \frac{c^2(\underline{s}^T\underline{h})^2}{c^2\,\underline{h}^T\Phi\,\underline{h}} \\ &= \frac{(\underline{s}^T\underline{h})^2}{\underline{h}^T\Phi\,\underline{h}} \\ &= OSNR \end{aligned} \tag{2.33}$$

Thus making the Lagrangian multiplier, λ, equal to 0.5 in equation (2.32) yields the impulse response of the MAMF which maximizes OSNR for a given Φ and $\underline{s}$. This impulse response, $\underline{\bar{h}}$, is given by

$$\underline{\bar{h}} = \Phi^{-1}\underline{s} \tag{2.34}$$

Substituting equation (2.34) into equation (2.29) yields the optimum OSNR, $OSNR_{opt}$,

$$\begin{aligned} OSNR_{opt} &= \frac{(\underline{s}^T\underline{\bar{h}})^2}{\underline{\bar{h}}^T\Phi\,\underline{\bar{h}}} \\ &= \frac{(\underline{s}^T\Phi^{-1}\underline{s})^2}{\underline{s}^T\Phi^{-1}\Phi\,\Phi^{-1}\underline{s}} \\ &= \underline{s}^T\Phi^{-1}\underline{s} \end{aligned} \tag{2.35}$$

Note that $OSNR_{opt}$ is a function of Φ and $\underline{s}$. From Section 2.1 and [CTC][KAB][WLB], Φ is NND, has real components, and so may be factored as follows

$$\Phi = U\Lambda U^T \tag{2.36}$$

where Λ is the canonical Jordan form diagonal matrix defined by

$$\Lambda = \begin{bmatrix} \lambda_0 & & 0 \\ & \lambda_1 & \\ & \vdots & \\ 0 & & \lambda_{N-1} \end{bmatrix} \tag{2.37}$$

and U is the modal matrix defined by

$$U = \left[\underline{u}_0 \mid \underline{u}_1 \mid \ldots \mid \underline{u}_{N-1} \right] \tag{2.38}$$

The eigenvectors $\underline{u}_0, \underline{u}_1, \ldots, \underline{u}_{N-1}$ are real since Φ is real and the i-th orthonormal eigenvector, $\underline{u}_i$, is associated with the i-th eigenvalue, λ_i. The eigenvalues are furthermore ordered as follows:

$$\lambda_0 \geq \lambda_1 \geq \cdots \geq \lambda_{N-1} \geq 0 \tag{2.39}$$

Letting $\underline{s}$ equal $\underline{u}_{N-1}$ and substituting this into equations (2.34) and (2.35) yields the maximum value of $OSNR_{opt}$, $OSNR_{\max}$, for a given colored noise. $OSNR_{\max}$ is derived as follows:

$$
\begin{aligned}
OSNR_{\max} &= \underline{s}^T \underline{h} \\
&= \underline{u}_{N-1}^T U \Lambda^{-1} U^T \underline{u}_{N-1} \\
&= \underline{u}_{N-1}^T \left[\underline{u}_0 \mid \underline{u}_1 \mid \ldots \mid \underline{u}_{N-1} \right] \Lambda^{-1} \left[\begin{array}{c} \underline{u}_0^T \\ \hline \underline{u}_1^T \\ \hline \vdots \\ \hline \underline{u}_{N-1}^T \end{array} \right] \underline{u}_{N-1} \\
&= \left[0 \ \ldots \ 0 \ 1 \right] \Lambda^{-1} \begin{bmatrix} 0 \\ \vdots \\ 0 \\ 1 \end{bmatrix} \\
&= \frac{1}{\lambda_{N-1}}
\end{aligned}
\tag{2.40}
$$

Therefore the maximum value for $OSNR_{opt}$, $OSNR_{\max}$, is equal to the inverse of the smallest eigenvalue of Φ. The signal vector which yields $OSNR_{\max}$ shall be called the optimal signal vector, $\underline{s}_{opt}$, and is equal to the eigenvector associated with the smallest eigenvalue. The impulse response for the MAMF which produces $OSNR_{\max}$, $\underline{h}_{opt}$, is defined

$$
\underline{h}_{opt} = \Phi^{-1} \underline{s}_{opt} = \Phi^{-1} \underline{u}_{N-1} \tag{2.41}
$$

Letting $\underline{s}$ equal $\underline{u}_0$ in equations (2.34) and (2.35) and proceeding as in equation (2.40) above produces the minimum value for OSNR, $OSNR_{\min} = \frac{1}{\lambda_0}$, which is the inverse of the largest eigenvalue of Φ .

2.5.4 Practical Performance

The developments of the preceeding section all assume that the noise autocorrelation, and hence the noise autocorrelation matrix Φ is known. For the practical case considered herein, the colored noise autocorrelation, Φ, is estimated and designated by $\Phi_{estimate}$. When Φ is estimated, $\underline{h}$ is not optimal and is given by,

$$\hat{\underline{h}} = \Phi_{estimate}^{-1} \underline{s} \tag{2.42}$$

Note furthermore that since the signal vectors are fixed prior to transmission, $\underline{s}$ is chosen either arbitrarily or on the basis of an expected colored noise. In either case, $\underline{s}$ may not be optimal. The OSNR for the practical implementation, $OSNR_{practical}$, wherein the autocorrelation of the colored noise is estimated and not known a priori and the signal vector is not optimal is derived by substituting equation (2.41) into equation (2.37)

$$\begin{aligned} OSNR_{practical} &= \frac{\left(\underline{s}^T \hat{\underline{h}}\right)^2}{\hat{\underline{h}}^T \Phi \hat{\underline{h}}} \\ &= \frac{\left(\underline{s}^T \Phi_{estimate}^{-1} \underline{s}\right)^2}{\underline{s}^T \Phi_{estimate}^{-1} \Phi \Phi_{estimate}^{-1} \underline{s}} \end{aligned} \tag{2.43}$$

Therefore since $\underline{s}$ and $\underline{h}$ are not necessarily equal to $\underline{s}_{opt}$ and $\underline{h}_{opt}$ respectively, $OSNR_{practical} \leq OSNR_{max}$.

An interesting characteristic of equation (2.43) is that the scaling of $\Phi_{estimate}$ scales $\hat{\underline{h}}$. It was shown in equation (2.33) that scaling the impulse response of the MAMF does not change the OSNR. Thus $\Phi_{estimate}$ can be scaled without affecting $OSNR_{practical}$. One advantage of this is that the estimated autocorrelation can be scaled to lessen the effects of rounding and truncation in an actual implementation.

Finally, the most crucial aspect of estimating the autocorrelation of the colored noise is that $OSNR_{max}$ can occur when $\Phi_{estimate} \neq \Phi$ while $\underline{s} = \underline{s}_{opt}$. To show this, first rewrite $\underline{h}_{opt}$ as a function of λ_{N-1} and $\underline{u}_{N-1}$:

$$\begin{aligned}
\underline{h}_{opt} &= \Phi^{-1}\,\underline{u}_{N-1} \\
&= U\,\Lambda^{-1}\,U^{T}\,\underline{u}_{N-1} \\
&= \left[\,\underline{u}_0 \mid \underline{u}_1 \mid \ldots \mid \underline{u}_{N-1}\,\right]\Lambda^{-1}\left[\begin{array}{c} \underline{u}_0^{T} \\ \hline \underline{u}_1^{T} \\ \hline \vdots \\ \hline \underline{u}_{N-1}^{T} \end{array}\right]\underline{u}_{N-1} \\
&= \frac{1}{\lambda_{N-1}}\,\underline{u}_{N-1}
\end{aligned} \tag{2.44}$$

Let Φ' be an estimated autocorrelation matrix for which $\underline{u}_{N-1}$ is an eigenvector and λ_{N-1} is not an eigenvalue, to insure $\Phi' \neq \Phi$, then

$$\begin{aligned}
\underline{h}' &= (\Phi')^{-1}\,\underline{u}_{N-1} \\
&= U'\,(\Lambda')^{-1}\,U'^{T}\,\underline{u}_{N-1} \\
&= \left[\,\underline{u}'_0 \mid \underline{u}'_1 \mid \ldots \mid \underline{u}'_{N-2} \mid \underline{u}_{N-1}\,\right](\Lambda')^{-1}\left[\begin{array}{c} \underline{u}'^{T}_0 \\ \hline \underline{u}'^{T}_1 \\ \hline \vdots \\ \hline \underline{u}'^{T}_{N-2} \\ \hline \underline{u}^{T}_{N-1} \end{array}\right]\underline{u}_{N-1} \\
&= \frac{1}{\lambda'_{N-1}}\,\underline{u}_{N-1} \\
&= c\,\frac{1}{\lambda_{N-1}}\,\underline{u}_{N-1} \\
&= c\,\underline{h}_{opt}
\end{aligned} \tag{2.45}$$

where c is a non-zero constant and λ'_{N-1} is not prime. From equation (2.33), multiplying $\underline{h}$ by an arbitrary constant does not change the value of OSNR, thus $\Phi' \neq \Phi$ produces a $OSNR = OSNR_{max}$. One must now prove the existence of Φ'.

There exist an infinite number of real symmetric Toeplitz matrices, Φ', that satisfy equation (2.45) provided $N > 2$. To prove this recall from Section 2.1 that the eigenvectors for a real symmetric Toeplitz matrix are or can be chosen to be either symmetric

$$\underline{u} = [u_0 \; u_1 \; \ldots \; u_1 \; u_0] \tag{2.46}$$

or skew-symmetric

$$\underline{u} = [u_0 \; u_1 \; \ldots \; -u_1 \; -u_0] \tag{2.47}$$

Consider the case where the eigenvector, $\underline{u}_{N-1}$, is symmetric. The skew-symmetric case is similar. The eigenvalue and eigenvector relationship for Φ' and $\lambda'_{N-1} \neq \lambda_{N-1}$ is written

$$\Phi' \underline{u}_{N-1} = \lambda'_{N-1} \underline{u}_{N-1}$$

$$\begin{bmatrix} \varphi_0 & \varphi_1 & \cdots & \varphi_{N-1} \\ \varphi_1 & \varphi_0 & \cdots & \varphi_{N-2} \\ \vdots & \vdots & \cdots & \vdots \\ \varphi_{N-2} & \varphi_{N-3} & \cdots & \varphi_1 \\ \varphi_{N-1} & \varphi_{N-2} & \cdots & \varphi_0 \end{bmatrix} \begin{bmatrix} u_0 \\ u_1 \\ \vdots \\ u_1 \\ u_0 \end{bmatrix} = \lambda'_{N-1} \begin{bmatrix} u_0 \\ u_1 \\ \vdots \\ u_1 \\ u_0 \end{bmatrix} \tag{2.48}$$

From the symmetry of Φ' and $\underline{u}_{N-1}$, equation (2.48) can be rewritten as follows:

$$\begin{bmatrix} u_0 & u_1 & \cdots & u_1 & u_0 \\ u_1 & u_0 + u_2 & \cdots & u_0 & 0 \\ \vdots & \vdots & \cdots & \vdots & \vdots \\ u_1 & u_0 + u_2 & \cdots & u_0 & 0 \\ u_0 & u_1 & \cdots & u_1 & u_0 \end{bmatrix} \begin{bmatrix} \varphi_0 \\ \varphi_1 \\ \vdots \\ \varphi_{N-2} \\ \varphi_{N-1} \end{bmatrix} = \lambda'_{N-1} \begin{bmatrix} u_0 \\ u_1 \\ \vdots \\ u_1 \\ u_0 \end{bmatrix} \tag{2.49}$$

Equation (2.49) can be written in matrix notation as

$$\hat{U}\underline{\varphi}' = \lambda'_{N-1}\,\underline{u}_{N-1} \tag{2.50}$$

Note that for N even, $\hat{U}$ will have $\frac{N}{2}$ identical rows, and for N odd, $\hat{U}$ will have $\frac{(N-1)}{2}$ identical rows provided $N > 2$. The identical rows in $\hat{U}$ make the linear system of equations in (2.50) underdetermined, and hence there exist an infinite number of solutions for $\underline{\varphi}'$. Therefore there are an infinite number of real symmetric Toeplitz matrices, Φ', that satisfy equation (2.45) provided $N > 2$.

The critical importance of $OSNR_{\max}$ occurring at points where $\Phi_{estimate} \neq \Phi$ is that the correlation estimator can produce an erronous estimate of the actual autocorrelation, with the MAMF receiver still producing an $OSNR = OSNR_{\max}$. Given that $\Phi_{estimate}$ is a function of the correlation estimator, $\Phi_{estimate}$ could posses the eigenvector $\underline{u}_{N-1}$ and hence $OSNR_{practical}$ could equal $OSNR_{\max}$ provided the transmitted signal vector $\underline{s}$ is equal to $\underline{u}_{N-1}$. In the traditional MAMF communication system wherein the signal vector is fixed, $OSNR_{estimate} = OSNR_{\max}$ only when the selected signal vector happens to equal $\underline{u}_{N-1}$ and $\underline{u}_{N-1}$ is an eigenvector of $\Phi_{estimate}$. Since the signal vector transmitted by the proposed MAMF communication system is composed of orthornormal basis vectors which span a sub-space **K**, $OSNR_{estimate} = OSNR_{\max}$ when $\underline{u}_{N-1}$ is in the sub-space **K** and $\underline{u}_{N-1}$ is an eigenvector of $\Phi_{estimate}$. Hence, as the color of the noise and the eigenvector

associated with the smallest eigenvalue changes, the $OSNR$ of the traditional MAMF receiver will not and cannot equal $OSNR_{max}$ while the $OSNR$ of the proposed system could equal $OSNR_{max}$. This is one advantage of the proposed MAMF communication system over the traditional MAMF communication system.

A second advantage of the proposed system is that $OSNR_{practical}$ and hence SNRI can be maximized for the combined estimated autocorrelation matrix $\Phi_{v\,estimate}$ and the signal vector sub-space **K** by proper choice of the linear combination coefficients c_i. In order to calculate the noise energy at the output of the MAMF one must know the actual combined autocorrelation matrix, Φ_{vv} thus $OSNR_{practical}$ cannot be maximized directly. The signal energy at the output of the MAMF can be computed, so one can attempt to maximize OSNR for the sub-space **K** by maximizing the signal energy out of the MAMF. Since the relationship between the c_i and the $OSNR_{practical}$ is highly non-linear due to the dependence of $OSNR_{practical}$ on the autocorrelation matrix $\Phi_{v\,estimate}$ and its eigenvectors, the signal energy out of the MAMF shall be maximized in order to maximize $OSNR_{practical}$ for the sub-space **K**.

3.0 Simulation and Results

The effects on performance of signal vector choice, different colored noise spectra, and estimation of the colored noise autocorrelation for both the proposed and traditional MAMF communication systems are investigated in this chapter. The investigation consists of performance comparisons between the proposed and traditional MAMF communication systems. Several cases are considered for each comparison and each case is presented graphically for ease of comparison. The general aspects of the systems and their simulations are discussed in the following sections.

3.1 Colored Noise

The additive colored Gaussian noise of the channel is produced by taking a Gaussian white noise process with a variance of 1.0 and coloring it with an Infinite Impulse Response (IIR) digital filter as depicted in Figure 6 on page 41. The Gaussian white noise process is generated using the IMSL routine GGNPM. The digital filter is

a narrowband digital filter with two dominant poles. The transfer function of the filter is

$$H(z) = \frac{b_1}{1 - 2\rho\cos(\theta)z^{-1} + \rho^2 z^{-2}} = \frac{b_1 z^2}{(z - \rho e^{j\theta})(z - \rho e^{-j\theta})} \tag{3.1}$$

where $\rho = 0.95$ and b_1 is defined such that the peak magnitude response is normalized to 1, i.e. $b_1 = (1 - \rho) \mid e^{j\theta} - \rho e^{-j\theta} \mid$. Thus $H(z)$ has two non-contributing zeros at $z = 0$ and two dominant poles at $z = \rho e^{\pm j\theta}$. From the z-plane pole-zero diagram of Figure 6 on page 41, ρ is the distance of the poles from the origin and so controls the bandwidth of the colored noise. Since $\rho = 0.95$ the noise is narrowband. The angle θ determines where the narrowband noise is centered. By changing the angle θ from 0 to π, the center frequency is swept from D.C. to one-half times the sampling frequency. The magnitude responses of the filter at $\theta = 0$ and $\frac{\pi}{2}$ are given in Figure 7 on page 42. Since the filter has an infinite impulse response, the first 2000 samples out of the noise coloring filter are discarded to avoid transient affects from influencing the colored noise samples and hence the autocorrelation estimates. The noise samples after the first 2000 are used to form the additive colored noise vectors.

Some of the cases discussed in this chapter use the actual autocorrelation of the colored noise for reasons to be discussed later. The actual autocorrelation of the colored noise is derived directly from the coefficients of the transfer function given in equation (3.1) using the method proposed by J.P. Dugre, A.A. Beex, and L.L. Scharf [DBS].

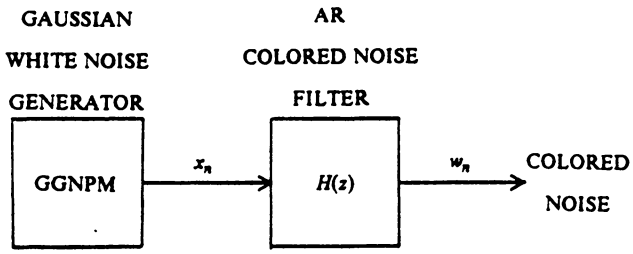

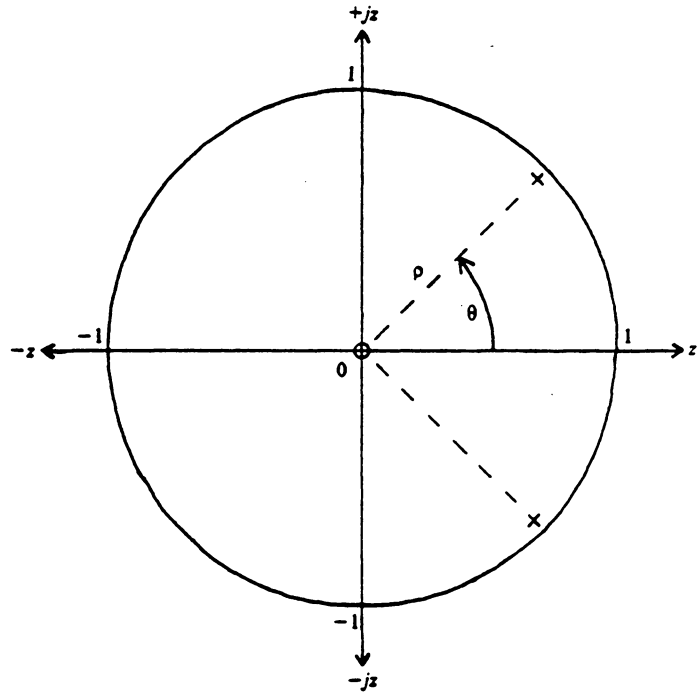

Figure 6. COLORED NOISE FILTER CHARACTERISTICS

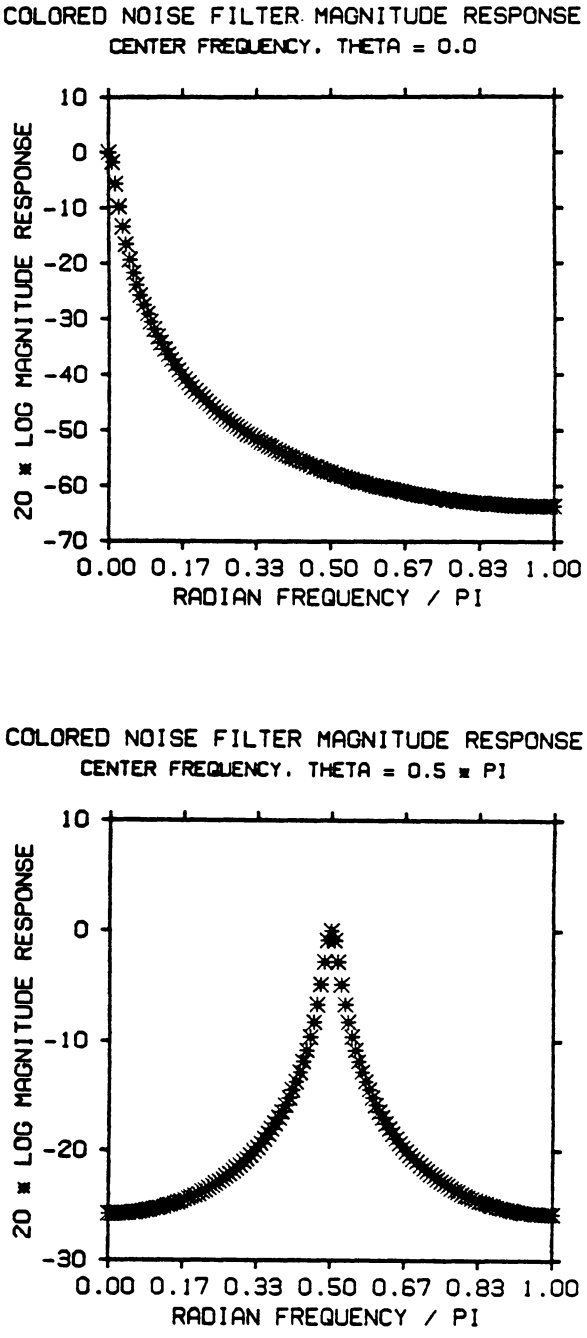

Figure 7. COLORED NOISE FILTER MAGNITUDE RESPONSE

3.2 *System Descriptions*

3.2.1 Proposed System

The objective of a MAMF communication system is to maximize the probability of detection and discrimination of known signal waveforms corrupted with colored noise. This is acomplished by maximizing the SNRI or performance. The signal vector for the proposed system was chosen to be of minimum length for binary data to emphasize the differences in performance between the proposed and traditional MAMF communication systems. From Section 2.3, the minimum number of linearly independent basis vectors required to span a sub-space is $K = 2$ and the minimum length of each basis vector for binary data, $p = 2$, is $K \times p = M = 4$. The M-dimensional linearly independent basis vectors selected are orthonormal and either symmetric or skew-symmetric. The transmitted signal vector is formed from the concatenation of the two orthonormal basis vectors and given by

$$\underline{s} = \left[\frac{\underline{s}_1}{\underline{s}_2} \right] \tag{3.2}$$

The length of the transmitted signal vector is thus $K \times M = N = 8$ The length of the signal vector for the traditional system shall also be of length $N = 8$ to make the comparison between the two systems fair. The length of the autocorrelation is $N = 8$, and so at least 8 noise samples are required to estimate the autocorrelation. The number of samples chosen to estimate the autocorrelation, i.e. the length of the vector containing the noise samples, is 16. The received signal, $\underline{I}$, composed of the transmitted signal of equation (3.2) and the additive colored noise, is given by

$$\underline{I} = [\underline{s}_1 + \underline{w}_1 \mid \underline{s}_2 + \underline{w}_2] \tag{3.3}$$

The length of $\underline{I}$ is 8 samples.

The advantage of the proposed system is that two orthonormal basis vectors are transmitted and by linearly combining them in the receiver, any signal vector in the 2-dimensional space can be constructed and used to maximize performance. Since $K = 2$ for the proposed system simulated herein, only two coefficients are needed to linearly combine the orthonormal basis vectors; furthermore, the signal energy of the transmitted signal for both systems is $E_s = 2$. From equation (2.11) the two coefficients, c_1 and c_2, must satisfy the following relationship:

$$\sum_{l=1}^{K} c_l^2 = c_1^2 + c_2^2 = E_s = 2 \tag{3.4}$$

Note that the points (c_1, c_2) lie along a circle of radius $\sqrt{2}$ on the $c_1 c_2$ plane. From equation (2.5), the signal vector resulting from the linear combination of the two orthonormal basis vectors is given by

$$\underline{\tilde{s}} = [\underline{s}_1 \mid \underline{s}_2] \begin{bmatrix} c_1 \\ c_2 \end{bmatrix} \tag{3.5}$$

From equations (2.19) and (3.4), the noise autocorrelation resulting from the linear combination of the colored noise vectors associated with the orthonormal basis vectors is given by

$$\begin{aligned} R_v(l) &= \left(c_1^2 + c_2^2\right) R_{ww}(l) + c_1 c_2 \left(R_{ww}(4 + l) + R_{ww}(4 - l)\right) \\ &= 2 R_{ww}(l) + c_1 c_2 \left(R_{ww}(4 + l) + R_{ww}(4 - l)\right) \end{aligned} \tag{3.6}$$

When the actual autocorrelation is known, the MAMF impulse response derived from equation (2.34) is

$$\underline{h} = \Phi_v^{-1} \underline{s} \tag{3.7}$$

The coefficients c_1 and c_2 are chosen to maximize OSNR. Since SNRI is maximized when OSNR is maximized, c_1 and c_2 are chosen to maximize OSNR. OSNR for the proposed system considered herein is derived from equation (2.23) as follows:

$$\begin{aligned} OSNR &= \frac{\left(\underline{s}^T \underline{h}\right)^2}{\underline{h}^T \Phi_v \underline{h}} \\ &= \frac{\left(\underline{s}^T \Phi_v^{-1} \underline{s}\right)^2}{\underline{s}^T \Phi_v^{-1} \Phi_v \Phi_v^{-1} \underline{s}} \\ &= \underline{s}^T \Phi_v^{-1} \underline{s} \end{aligned} \tag{3.8}$$

The coefficients c_1 and c_2 which maximize equation (3.8) are henceforth referred to as the optimum coefficients $c_{1\,opt}$ and $c_{2\,opt}$ respectively.

When the noise autocorrelation is not known and must be estimated, the estimated autocorrelation matrix, $\Phi_{estimate}$, is not necessarily equal to the actual autocorrelation matrix, Φ; furthermore, the autocorrelation matrix of the combined noise formed from $\Phi_{estimate}$ and designated by $\Phi_{v\,estimate}$, is not necessarily equal to the autocorrelation of the combined noise formed from the actual autocorrelation matrix Φ_v. The impulse response of the MAMF is derived from equation (2.37) to be

$$\hat{\underline{h}} = \Phi_{v\,estimate}^{-1} \underline{s} \tag{3.9}$$

The OSNR of the proposed system is derived from equation (2.38) as follows:

$$OSNR = \frac{\left(\underline{\tilde{s}}^T \underline{\hat{h}}\right)^2}{\underline{\hat{h}}^T \Phi_{v\,estimate}^{-1} \underline{\hat{h}}} = \frac{\left(\underline{\tilde{s}}^T \Phi_{v\,estimate}^{-1} \underline{\tilde{s}}\right)^2}{\underline{\tilde{s}}^T \Phi_{v\,estimate}^{-1} \Phi_v \Phi_{v\,estimate}^{-1} \underline{\tilde{s}}} \tag{3.10}$$

Note that when the noise characteristics are estimated and not known, the noise energy at the output of the MAMF cannot be computed. Thus OSNR and SNRI cannot be maximized directly to obtain $c_{1\,opt}$ and $c_{2\,opt}$. Since the signal energy at the output of the MAMF can be computed with the estimated noise autocorrelation, OSNR and SNRI shall be maximized by maximizing the signal energy at the output of the MAMF which is derived from equation (2.27) as follows:

$$E_{\tilde{s}} = \left(\underline{\tilde{s}}^T \underline{\hat{h}}\right)^2 = \left(\underline{\tilde{s}}^T \Phi_{v\,estimate}^{-1} \underline{\tilde{s}}\right)^2 \tag{3.11}$$

The coefficients which maximize equation (3.11) shall henceforth be referred to as $c'_{1\,opt}$ and $c'_{2\,opt}$. Note that as $\Phi_{v\,estimate}$ approaches Φ_v, $c'_{1\,opt}$ and $c'_{2\,opt}$ approach $c_{1\,opt}$ and $c_{2\,opt}$ and $E_{\tilde{s}}$ approaches $OSNR^2$, thus the accuracy of the maximization is a function of the estimator. The maximization of equation (3.11) was performed using a brute force approach wherein c_1 was varied from $-\sqrt{2}$ to $\sqrt{2}$ by increments of $(2\sqrt{2})/1000$ and c_2 was calculated from c_1 by $c_2 = \sqrt{2 - c_1^2}$.

3.2.2 Traditional System

In order to keep the comparisons between the proposed and traditional MAMF communication systems fair, the transmitted signal vector of the traditional system, $\underline{s}$,

has length $N = 8$. The received transmission, $\underline{I}$, composed of the transmitted signal vector with additive colored noise is represented as follows:

$$\underline{I} = [\underline{s} + \underline{w}] \tag{3.12}$$

where the length of $\underline{I}$ is 16.

The OSNR for the traditional system is given by equation (2.29) and repeated here:

$$OSNR = \frac{(\underline{s}^T \underline{h})^2}{\underline{h}^T \Phi \underline{h}} \tag{3.13}$$

where $\underline{h}$ is the impulse response of the MAMF. When the colored noise autocorrelation is known, $\underline{h}$ is given by equation (2.34) to be

$$\underline{h} = \Phi^{-1} \underline{s} \tag{3.14}$$

and the OSNR is optimum, $OSNR_{opt}$, and given by equation (2.29) to be

$$OSNR_{opt} = \underline{s}^T \Phi^{-1} \underline{s} \tag{3.15}$$

When the colored noise autocorrelation is estimated, $\underline{h}$, is given by equation (2.37) to be

$$\hat{\underline{h}} = \Phi_{estimate}^{-1} \underline{s} \tag{3.16}$$

and OSNR is representative of the practical situation considered herein, $OSNR_{practical}$, and given by equation (2.38) to be

$$OSNR_{practical} = \frac{(\underline{s}^T \Phi_{estimate}^{-1} \underline{s})^2}{\underline{s}^T \Phi_{estimate}^{-1} \Phi \Phi_{estimate}^{-1} \underline{s}} \tag{3.17}$$

3.3 Comparison Descriptions

The first comparison investigates the maximum SNRI for both the traditional and proposed MAMF communication systems. The normalized center frequency of the narrowband colored noise is swept from $\theta = 0$ to π at the discrete points $\theta = n\frac{\pi}{100}$, where $n = 0, 1, \ldots, 100$, and the maximum performance, in terms of SNRI, is computed in decibels (dB) at each point. Since SNRI is maximum for maximum OSNR, maximum OSNR is computed at each point. From equation (2.40), the maximum OSNR, $OSNR_{max}$, is equal to the inverse of the smallest eigenvalue of the real symmetric Toeplitz colored noise autocorrelation matrix. The noise autocorrelation sequence, R_{ww}, is computed rather than estimated at each of the discrete colored noise points. The maximum SNRI for the traditional system is computed by taking the inverse of the minimum eigenvalue of the 8×8 noise autocorrelation matrix, Φ, formed from R_{ww}. The 4×4 noise autocorrelation matrix for the proposed system, Φ_v, is a function of R_{ww}, which is fixed for a given colored noise, and the coefficients c_1 and c_2. The $OSNR_{max}$ for the proposed system occurs when the smallest eigenvalue of Φ_v is minimized. The coefficients c_1 and c_2 are varied in accordance with equation (3.4) to minizize the smallest eigenvalue of Φ_v and produce $OSNR_{max}$ and maximum SNRI. The results are graphically presented in Figure 8 on page 53.

The second comparison is between the traditional system optimized to produce the maximum OSNR, $OSNR_{max}$, for the colored noise at specific center frequencies, θ's, and the proposed system which used both symmetric and anti-symmetric orthonormal basis vectors. The traditional system was optimized in the first two cases for colored noise with normalized center frequency $\theta = 0$ and in the second two cases $\theta = \frac{\pi}{2}$. The signal vector of the traditional system was thus fixed in each case to be the eigenvector

associated with the minimum eigenvalue of the colored noise autocorrelation matrix at each of the normalized center frequencies. The orthonormal basis vectors used to compose the signal vector for the proposed system were fixed in the first and third cases to be symmetric

$$\begin{aligned} \underline{s}_1 &= \left[\frac{\sqrt{2}}{2} \; 0 \; 0 \; \frac{\sqrt{2}}{2}\right] \\ \underline{s}_2 &= \left[0 \; \frac{\sqrt{2}}{2} \; \frac{\sqrt{2}}{2} \; 0\right] \end{aligned} \tag{3.18}$$

and in the second and fourth cases to be skew-symmetric

$$\begin{aligned} \underline{s}_1 &= \left[\frac{\sqrt{2}}{2} \; 0 \; 0 \; -\frac{\sqrt{2}}{2}\right] \\ \underline{s}_2 &= \left[0 \; \frac{\sqrt{2}}{2} \; -\frac{\sqrt{2}}{2} \; 0\right] \end{aligned} \tag{3.19}$$

The transmitted signal energy for the traditional system was equal to the transmitted signal energy of the proposed system which is equal to 2 to keep the comparisions fair. The normalized center frequency of the narrowband colored noise was swept from $\theta = 0$ to π at discrete points as in the first comparison. The colored noise autocorrelation at each of the discrete points is calculated rather than estimated. In using the actual autocorrelation, one can observe the behavior of the traditional system as the noise varies under ideal conditions from the optimized noise center frequencies. From the conclusions of Section 2.5, the performance of either of the systems can reach a maximum for other actual autocorrelations. Thus the use of the actual autocorrelaion shall also provide insight into the performance of both systems for the case where the estimators are 100% accurate and can be used to contrast the performance of both systems when the autocorrelation is estimated. The performance, in terms of SNRI, was computed in decibels (dB) for both systems at each of the discrete colored noise points.

The results of each of the four cases are graphically presented in Figure 9 on page 54, Figure 10 on page 55, Figure 11 on page 56, and Figure 12 on page 57.

In the third comparison, the traditional system is not optimized for any particular colored noise. The signal vector of the traditional system was fixed in the first case to be the symmetric vector

$$\underline{s} = \left[\frac{\sqrt{2}}{2}\ 0\ \frac{\sqrt{2}}{2}\ 0\ 0\ \frac{\sqrt{2}}{2}\ 0\ \frac{\sqrt{2}}{2}\right] \tag{3.20a}$$

in the second case it was fixed to be the skew-symmetric vector

$$\underline{s} = \left[\frac{\sqrt{2}}{2}\ 0\ \frac{\sqrt{2}}{2}\ 0\ 0\ -\frac{\sqrt{2}}{2}\ 0\ -\frac{\sqrt{2}}{2}\right] \tag{3.20b}$$

in the third case it was fixed to be the symmetric vector

$$\underline{s} = \left[\frac{\sqrt{2}}{2}\ 0\ 0\ \frac{\sqrt{2}}{2}\ 0\ \frac{\sqrt{2}}{2}\ \frac{\sqrt{2}}{2}\ 0\right] \tag{3.21a}$$

and in the fourth case it was fixed to be the skew-symmetric vector

$$\underline{s} = \left[\frac{\sqrt{2}}{2}\ 0\ 0\ -\frac{\sqrt{2}}{2}\ 0\ \frac{\sqrt{2}}{2}\ -\frac{\sqrt{2}}{2}\ 0\right] \tag{3.21b}$$

The signal vector for the proposed system was fixed to be in the first and third cases symmetric and in the second and fourth cases skew-symmetric as given in equations (3.18) and (3.19) respectively. Note that again the transmitted signal energy of the traditional system is equal to the transmitted signal energy of the proposed system to keep the comparisons fair. The actual colored noise autocorrelation was again used for reasons previously discussed. The center frequency of the colored noise was swept swept from $\theta = 0$ to $\theta = \pi$ as in the first comparison. The performance, in terms of SNRI (dB), was computed for both systems at each of the discrete colored noise points. The

results of each of the four cases are graphically presented in Figure 13 on page 58, Figure 14 on page 59, Figure 15 on page 60, and Figure 16 on page 61.

In the fourth and last comparison, the colored noise autocorrelation was estimated. In the first two cases the autocorrelation was estimated with the classical biased estimator and in the second two cases by the Burg estimator. The signal vectors for the traditional and proposed systems were fixed in the first and third cases to be symmetric as given in equations (3.20a) and (3.18) respectively and in the second and fourth cases fixed to be skew-symmetric as given in equations (3.20b) and (3.19) respectively. Since the autocorrelation was estimated, the estimated autocorrelations were stochastic and hence so was the performance for both systems. The center frequency of the narrowband colored noise was changed to seven discrete frequencies, $\theta = n\frac{\pi}{7}$, where $n = 0, 1, \ldots, 7$. The autocorrelation was estimated and the SNRI (dB) computed one thousand times at each of the seven discrete colored noise points. The maximum SNRI (rounded to the nearest integer value), average SNRI, and average SNRI minus the standard deviation were computed for each system at each of the seven colored noises. The results of all four cases are graphically represented in Figure 17 on page 62, Figure 18 on page 63, Figure 19 on page 64 and Figure 20 on page 65.

3.4 Comparison Data

The following figures were generated on the Versatec plotter using the software package Nagplot at VPI & SU.

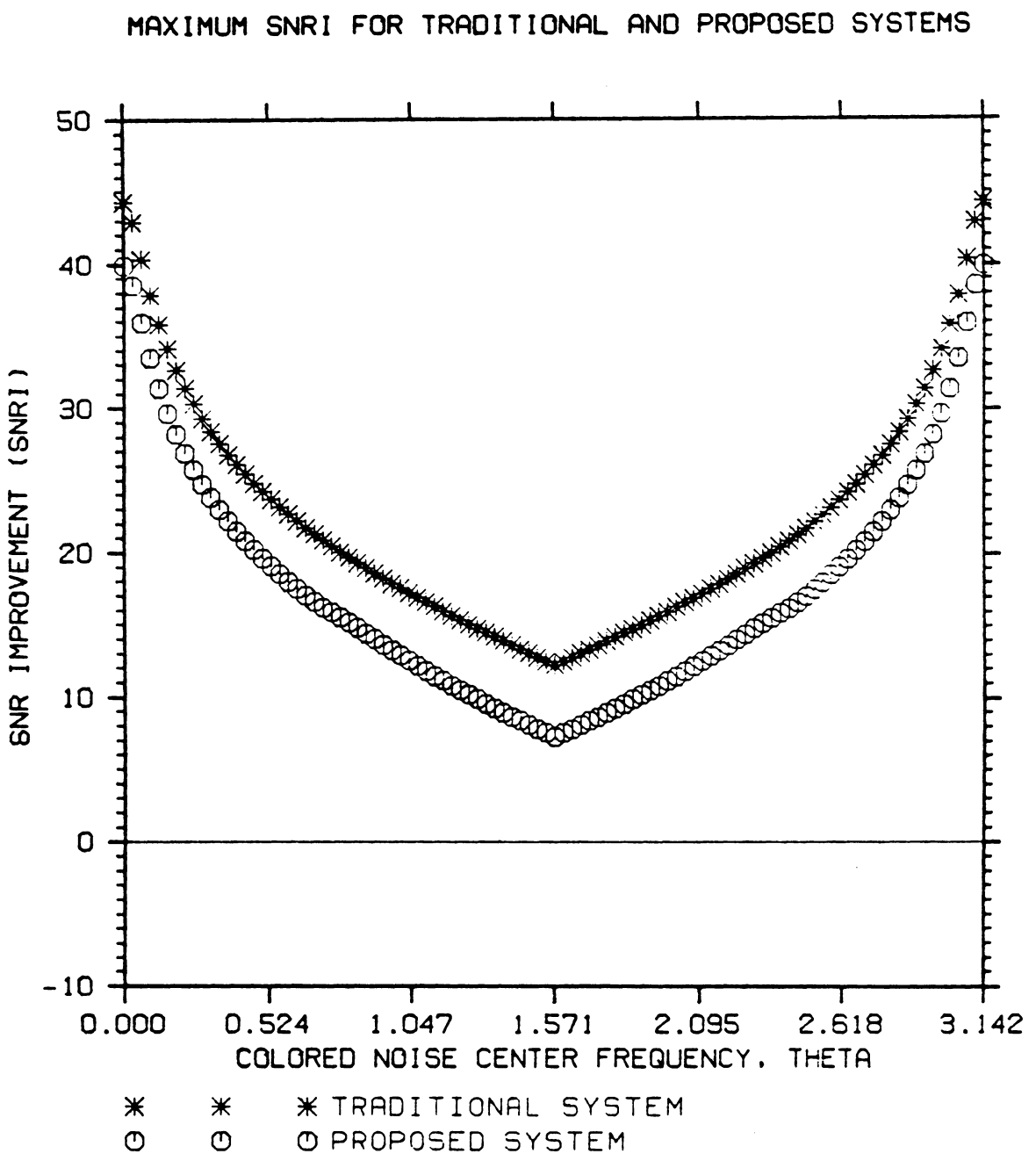

Figure 8. COMPARISON 1: MAXIMUM SNRI FOR BOTH THE TRADITIONAL AND PROPOSED MAMF COMMUNICATION SYSTEMS OVER VARIOUS NOISE COLORS

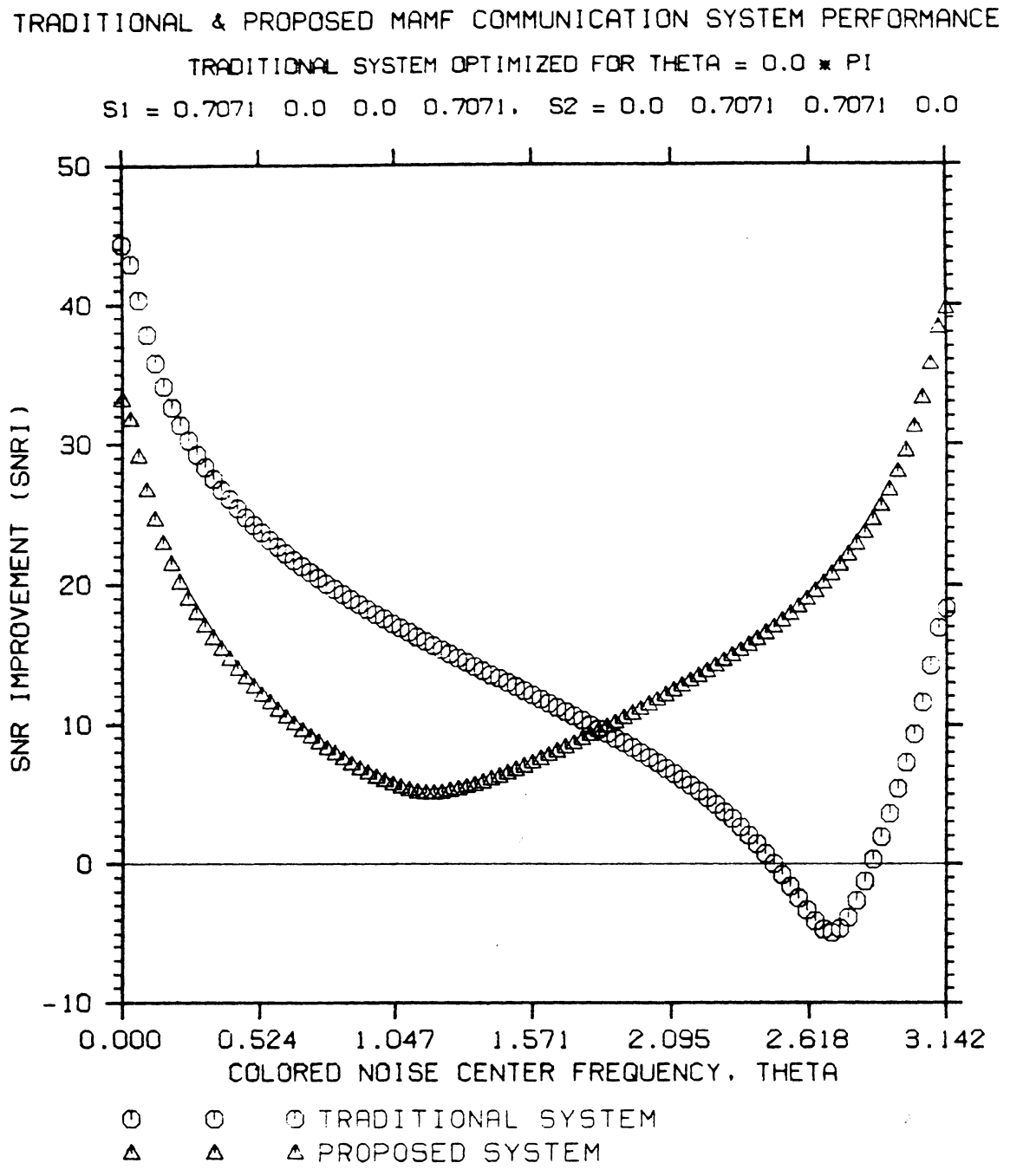

Figure 9. COMPARISON 2, CASE 1: TRADITIONAL SYSTEM OPTIMIZED AT $\theta = 0$, PROPOSED SYSTEM SIGNAL VECTOR is SYMMETRIC

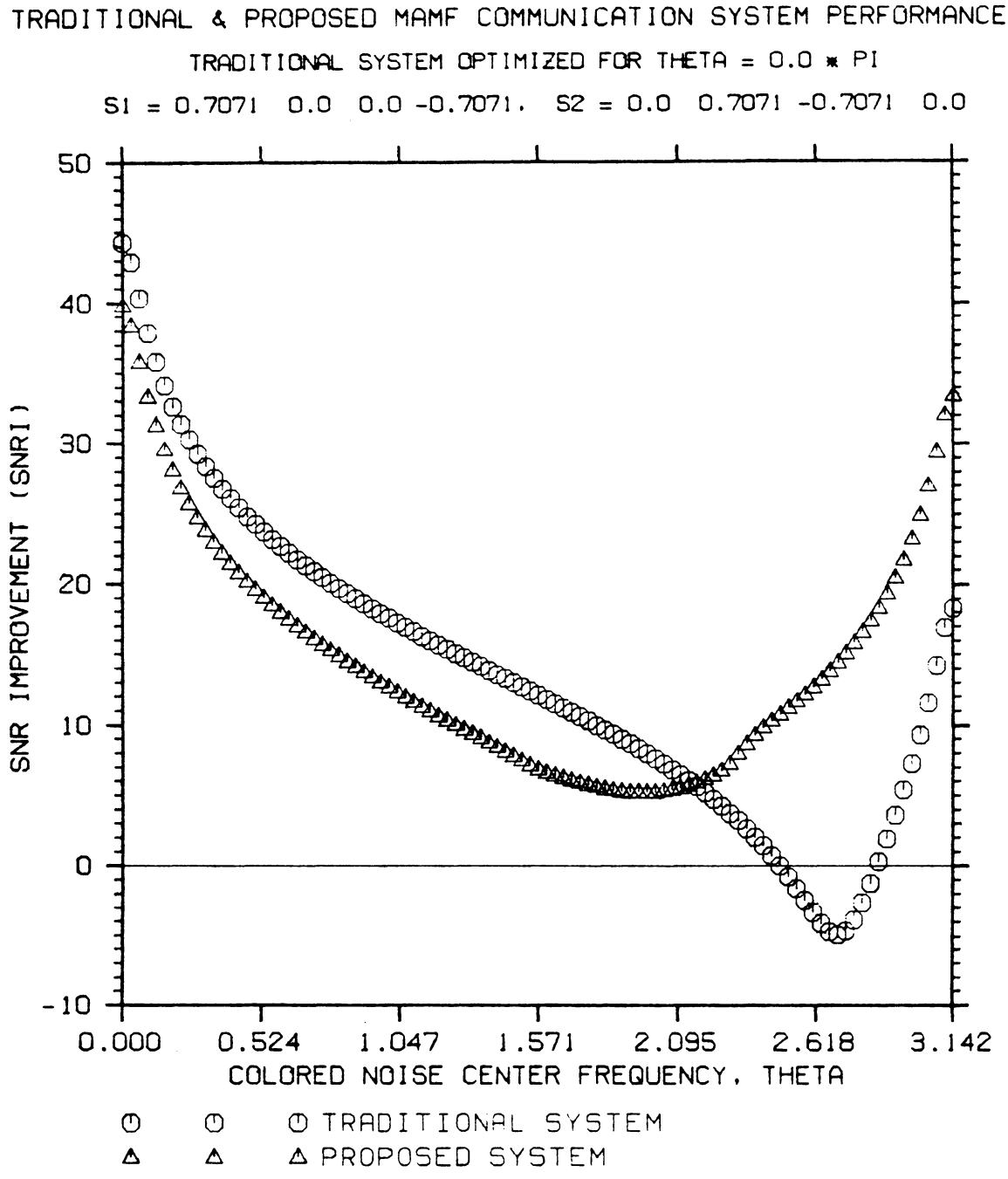

Figure 10. COMPARISON 2, CASE 2: TRADITIONAL SYSTEM OPTIMIZED AT $\theta = 0$, PROPOSED SYSTEM SIGNAL VECTOR is SKEW-SYMMETRIC

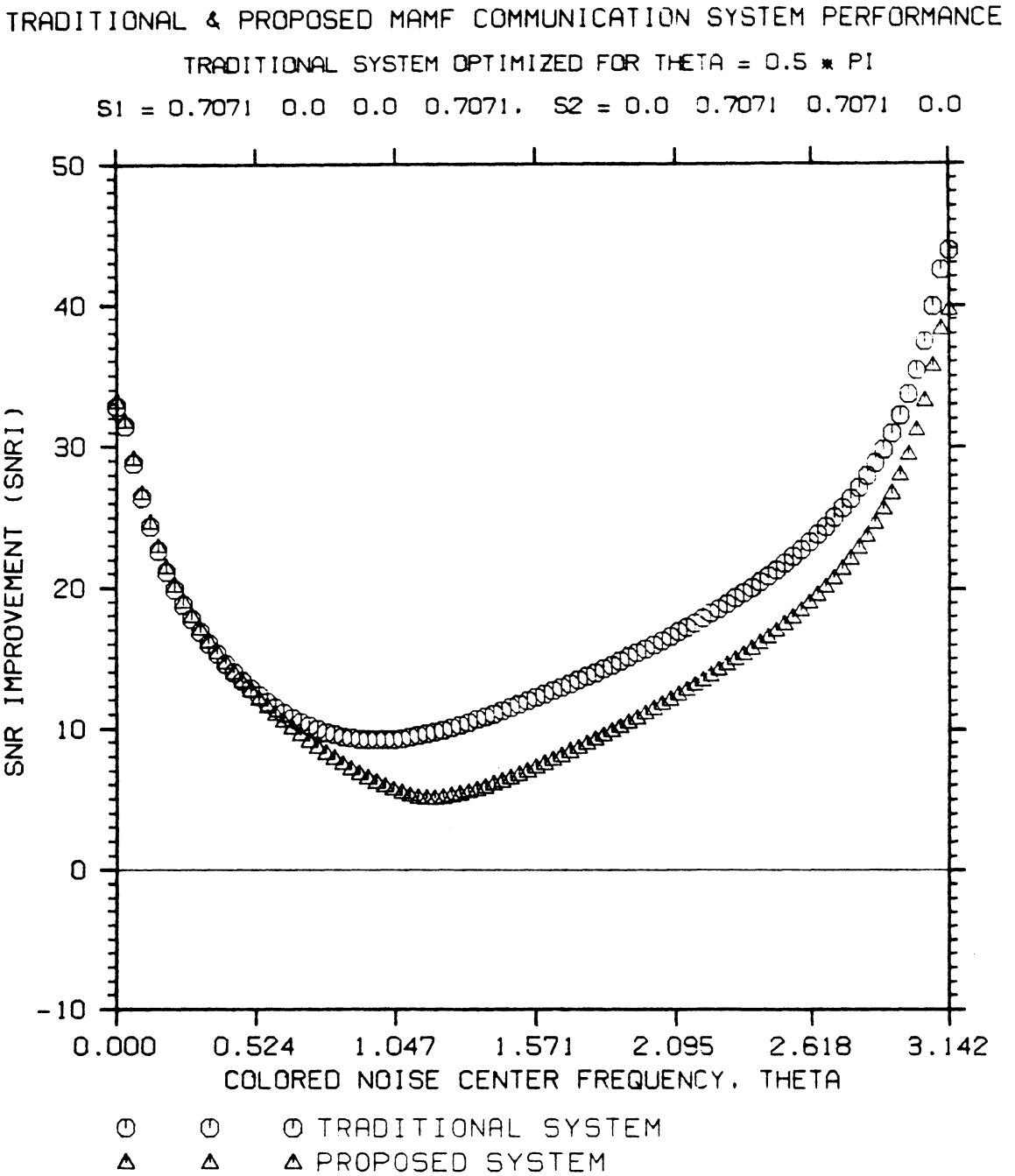

Figure 11. COMPARISON 2, CASE 3: TRADITIONAL SYSTEM OPTIMIZED AT $\theta = \frac{\pi}{2}$, PROPOSED SYSTEM SIGNAL VECTOR is SYMMETRIC

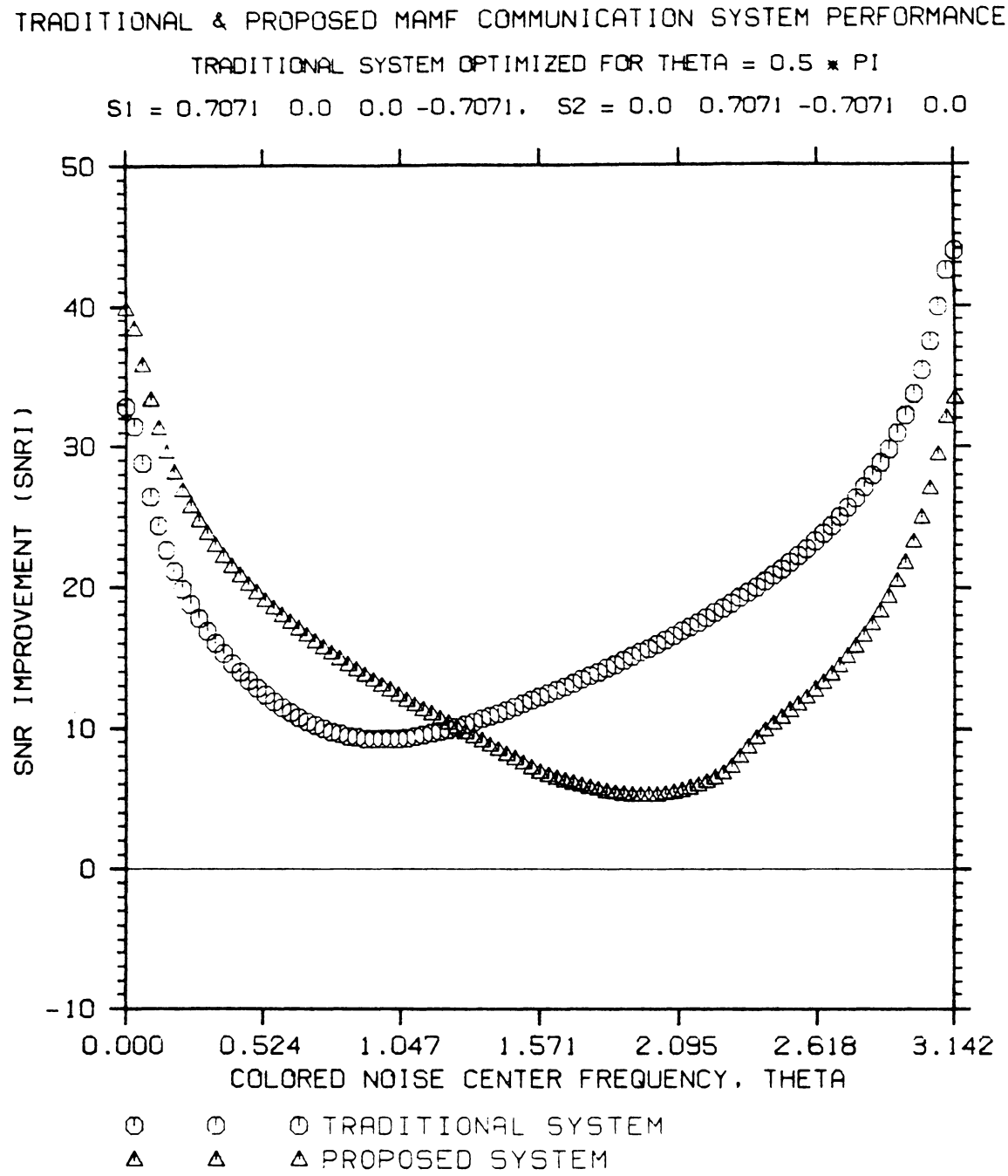

Figure 12. COMPARISON 2, CASE 4: TRADITIONAL SYSTEM OPTIMIZED AT $\theta = \frac{\pi}{2}$, PROPOSED SYSTEM SIGNAL VECTOR is SKEW-SYMMETRIC

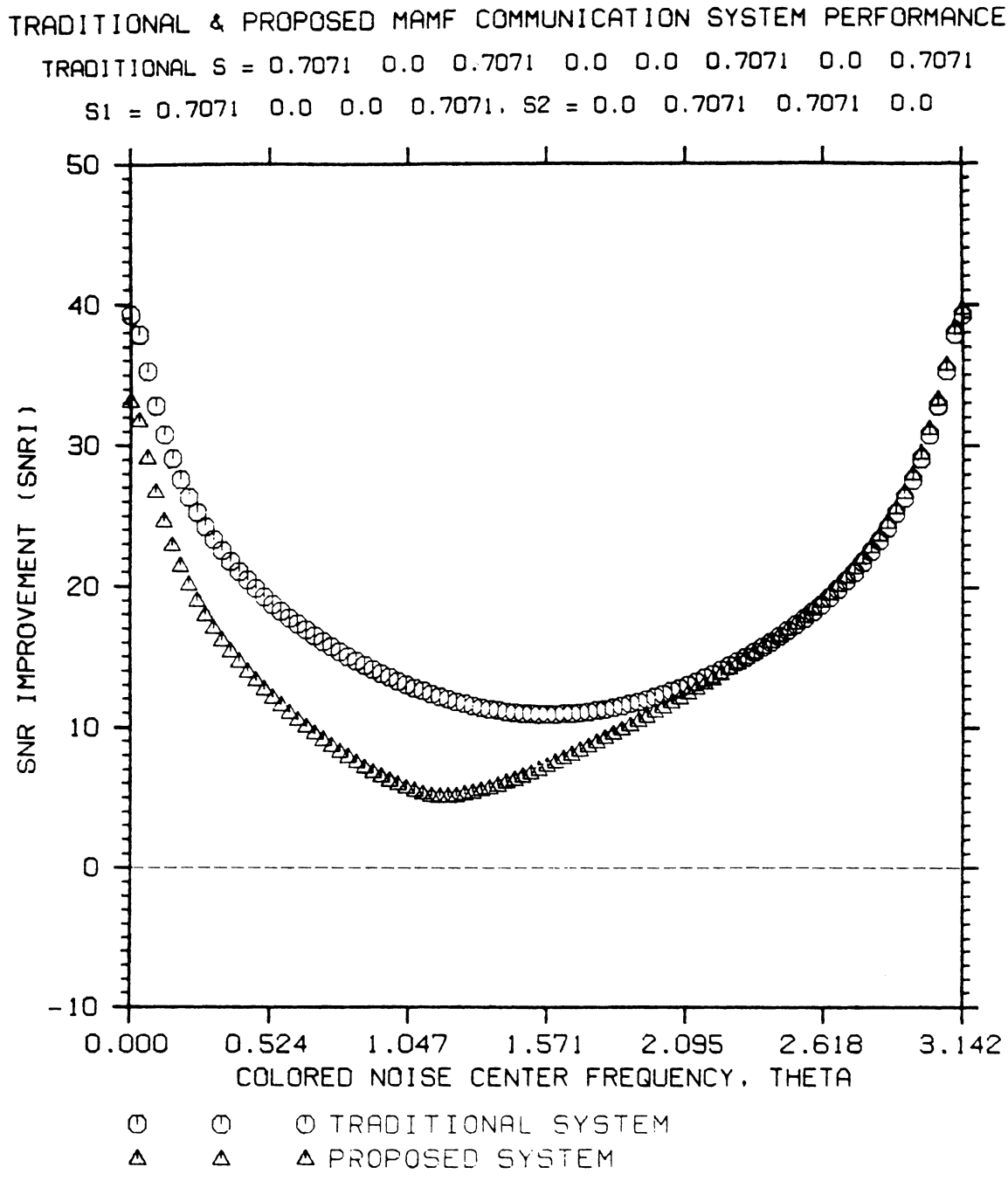

Figure 13. COMPARISON 3, CASE 1: TRADITIONAL and PROPOSED SYSTEM SIGNAL VECTORS are SYMMETRIC

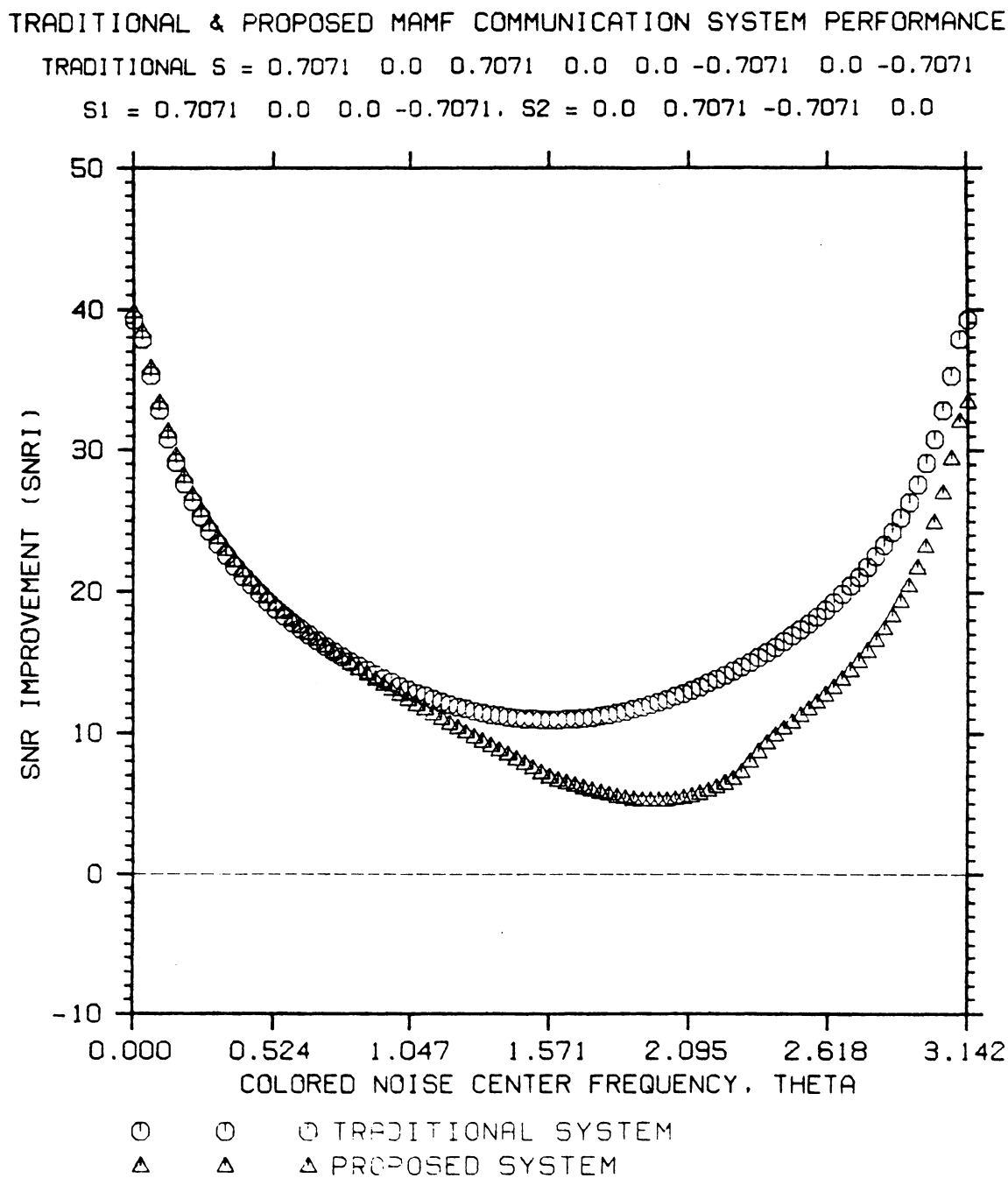

Figure 14. COMPARISON 3, CASE 2: TRADITIONAL SYSTEM SIGNAL VECTOR is SKEW-SYMMETRIC and PROPOSED SYSTEM SIGNAL VECTOR is SYMMETRIC

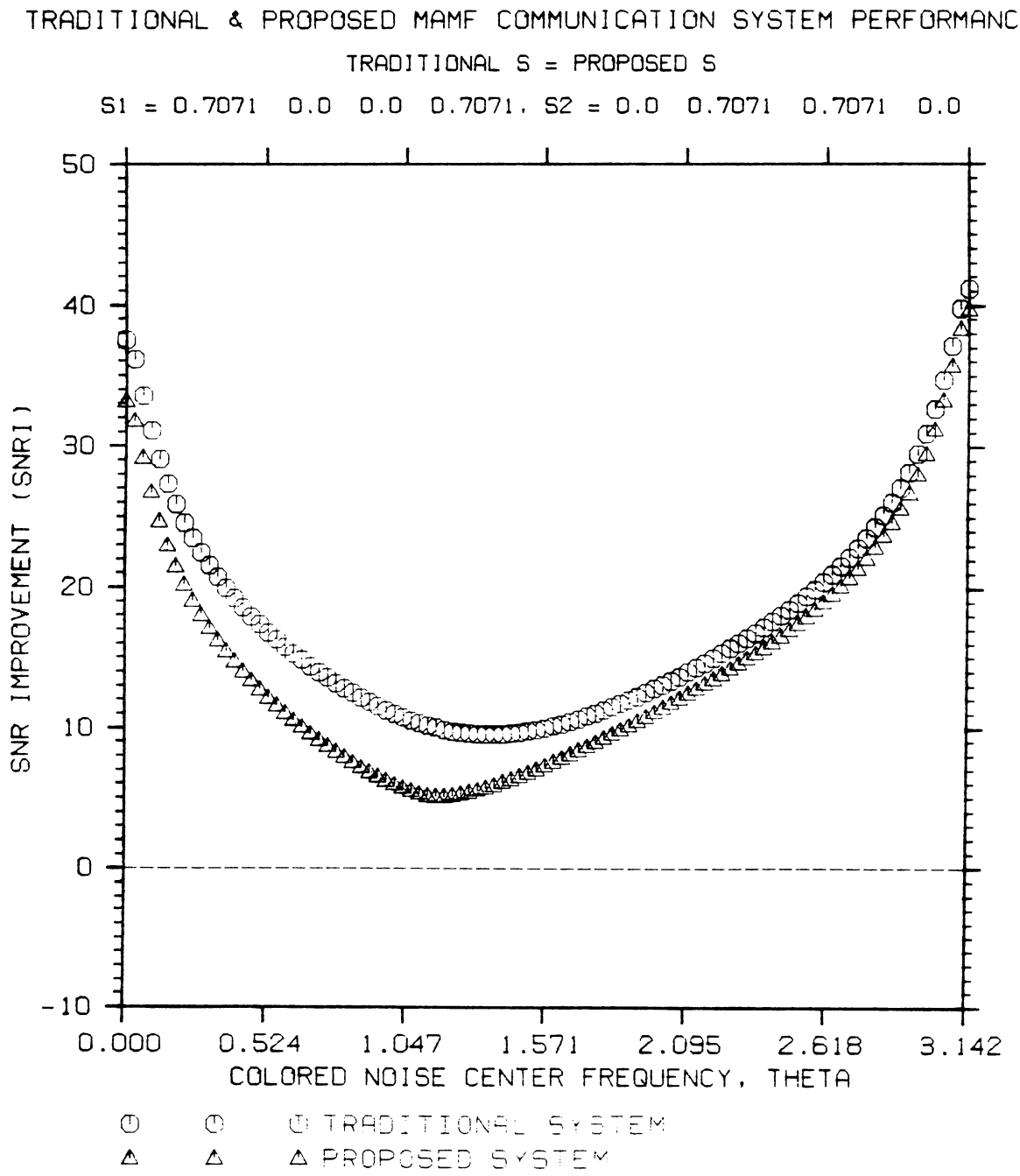

Figure 15. COMPARISON 3, CASE 3: TRADITIONAL SYSTEM SIGNAL VECTOR is SYMMETRIC and PROPOSED SYSTEM SIGNAL VECTOR is SKEW-SYMMETRIC

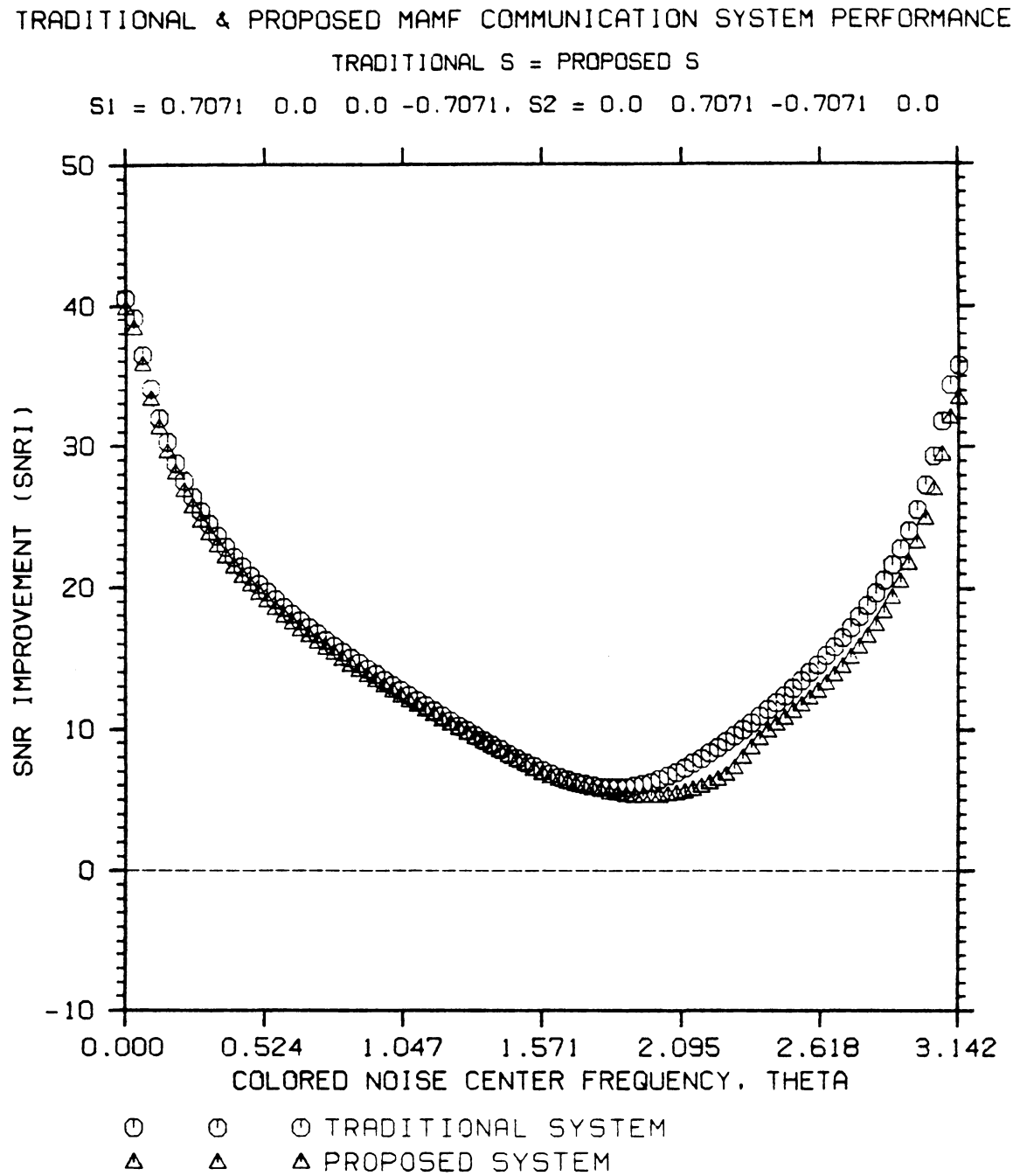

Figure 16. COMPARISON 3, CASE 4: TRADITIONAL and PROPOSED SYSTEM SIGNAL VECTORS are SKEW-SYMMETRIC

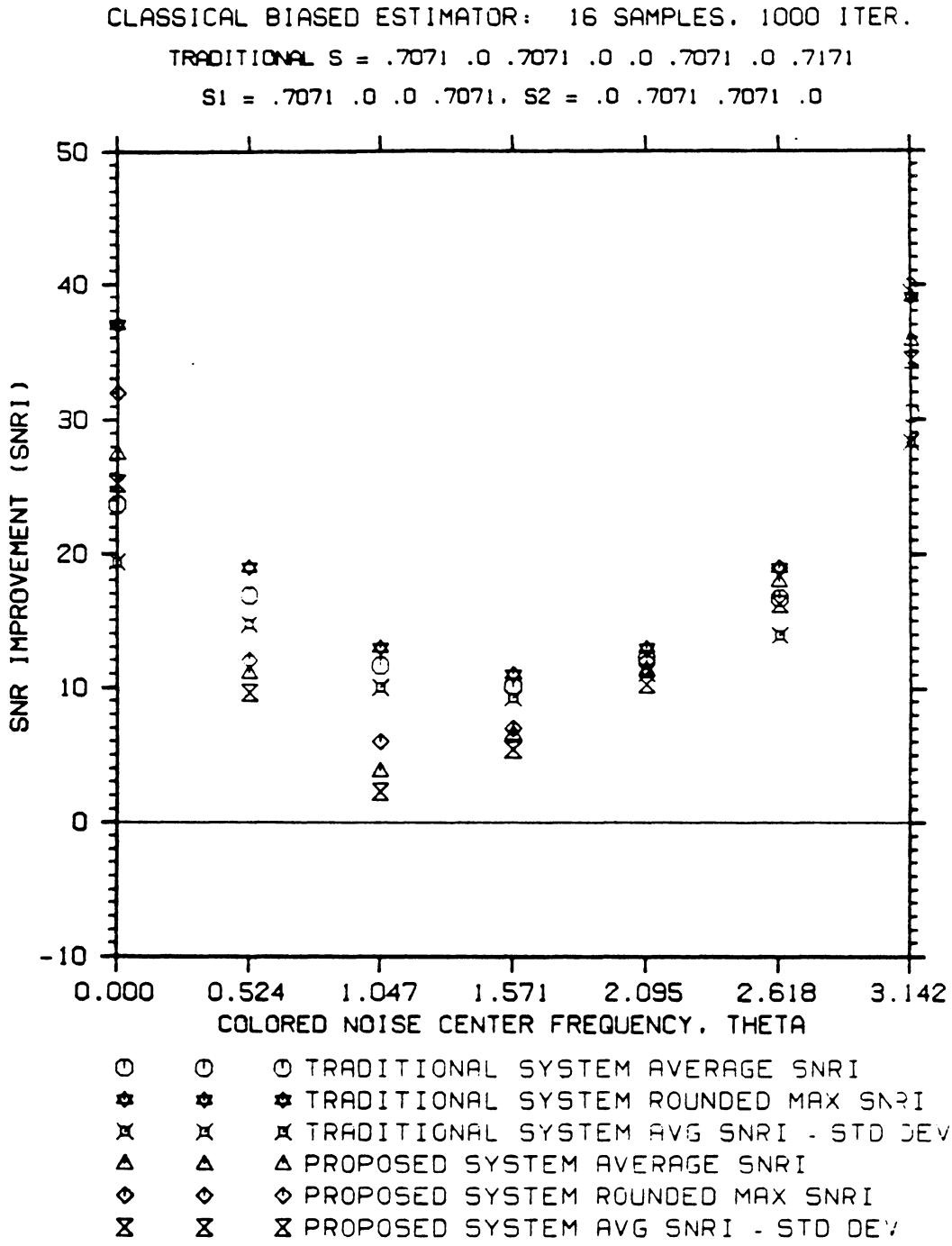

Figure 17. COMPARISON 4, CASE 1: TRADITIONAL and PROPOSED SYSTEM SIGNAL VECTORS are SYMMETRIC; CLASSICAL BIASED ESTIMATOR w/ 16 SAMPLES and 1000 ITERATIONS

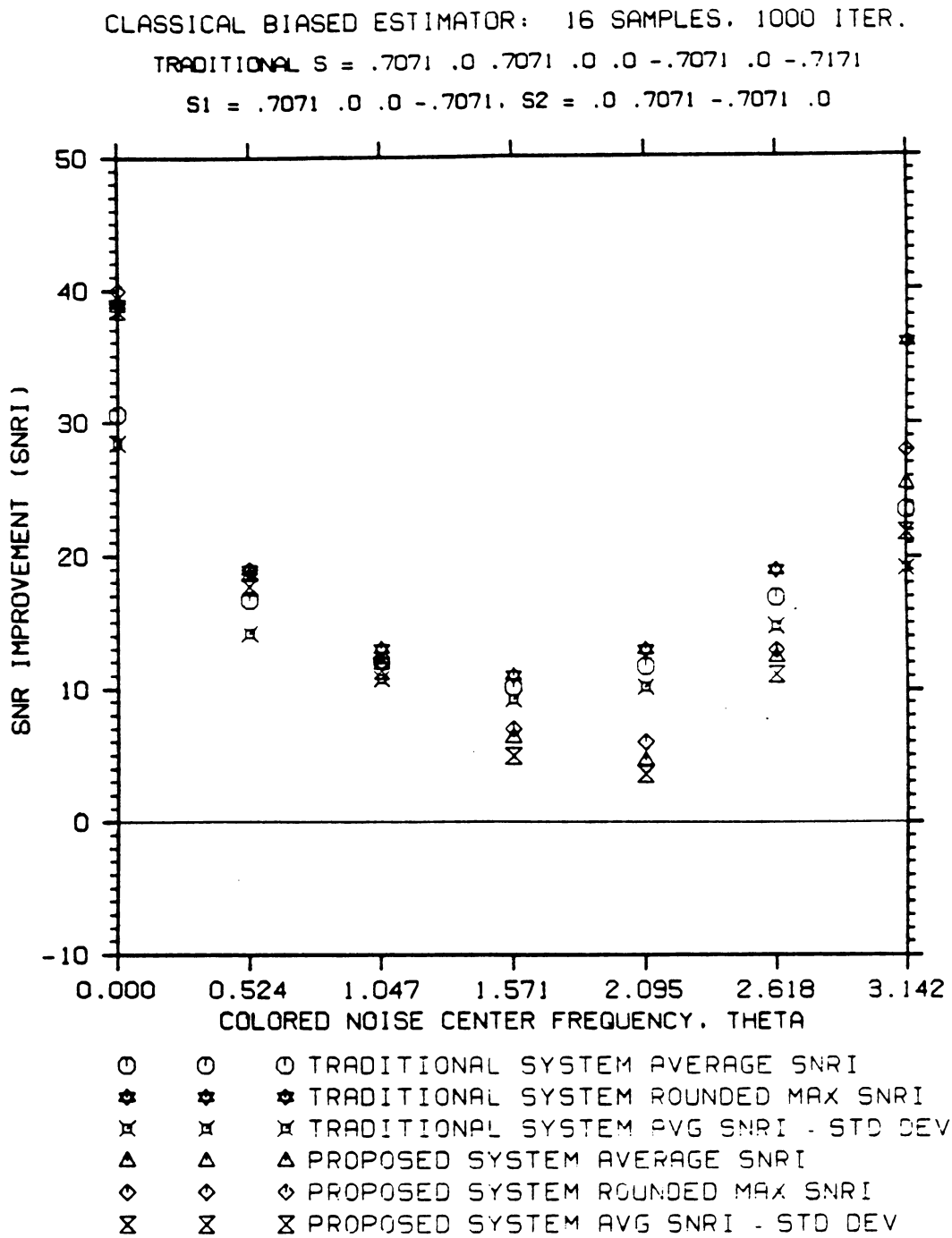

Figure 18. COMPARISON 4, CASE 2: TRADITIONAL and PROPOSED SYSTEM SIGNAL VECTORS are SKEW-SYMMETRIC; CLASSICAL BIASED ESTIMATOR w/ 16 SAMPLES and 1000 ITERATIONS

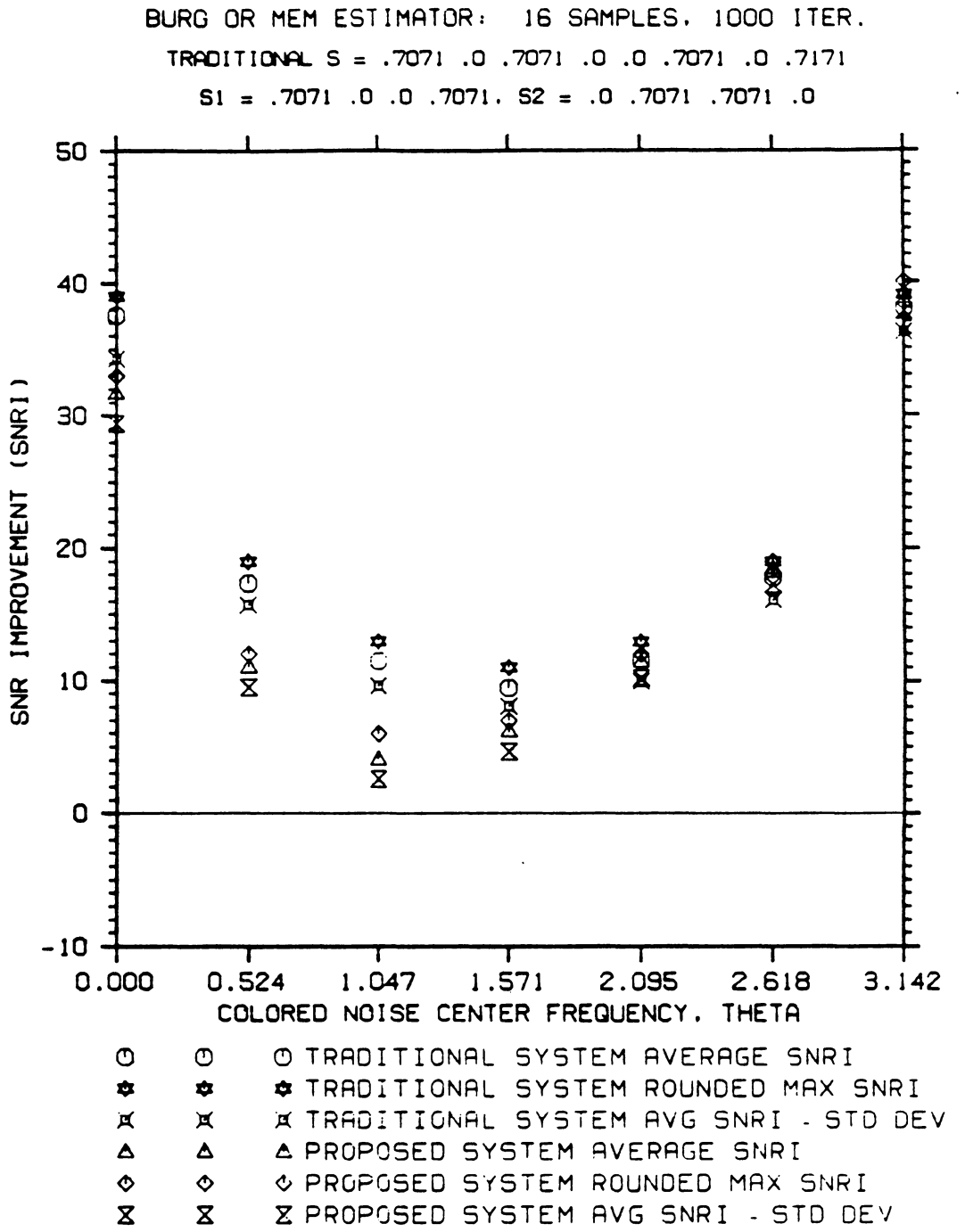

Figure 19. COMPARISON 4, CASE 3: TRADITIONAL and PROPOSED SYSTEM SIGNAL VECTORS are SYMMETRIC; BURG ESTIMATOR w/ 16 SAMPLES and 1000 ITERATIONS

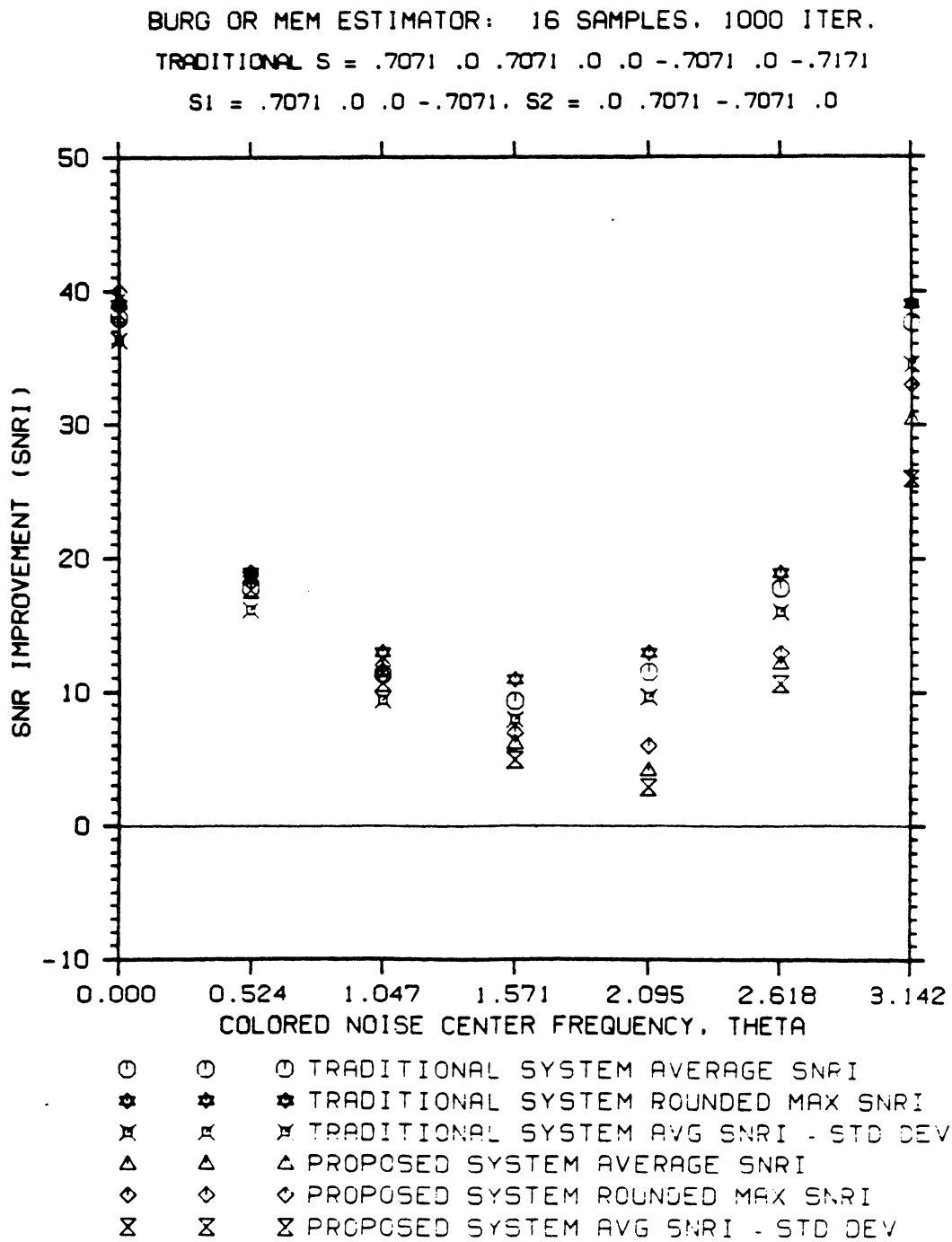

Figure 20. COMPARISON 4, CASE 4: TRADITIONAL and PROPOSED SYSTEM SIGNAL VECTORS are SKEW-SYMMETRIC; BURG ESTIMATOR w/ 16 SAMPLES and 1000 ITERATIONS

Table 1. Tabulated Statistical SNRI Data for Figure 17

Traditional System, CB Estimator, Symmetric Signal Vectors

SNRI Stats.	Theta 0.000	0.524	1.047	1.571	2.095	2.618	3.142
Maximum	37.0	19.0	13.0	11.0	13.0	19.0	39.0
Average	23.720	16.910	11.656	10.117	12.133	16.689	30.445
Std Dev	4.294	2.207	1.614	0.852	1.027	2.734	2.113

Proposed System, CB Estimator, Symmetric Signal Vectors

SNRI Stats.	Theta 0.000	0.524	1.047	1.571	2.095	2.618	3.142
Maximum	32.0	12.0	6.0	7.0	12.0	19.0	40.0
Average	27.512	11.088	3.841	6.554	11.410	17.971	35.877
Std Dev	2.259	1.470	1.547	1.131	1.137	1.684	1.463

Table 2. Tabulated Statistical SNRI Data for Figure 18

Traditional System, CB Estimator, Skew-symmetric Signal Vectors

SNRI Stats.	Theta 0.000	0.524	1.047	1.571	2.095	2.618	3.142
Maximum	39.0	19.0	13.0	11.0	13.0	19.0	36.0
Average	30.603	16.675	12.020	10.115	11.696	16.953	23.525
Std Dev	2.132	2.518	1.291	0.875	1.564	2.145	4.362

Proposed System, CB Estimator, Skew-symmetric Signal Vectors

SNRI Stats.	Theta 0.000	0.524	1.047	1.571	2.095	2.618	3.142
Maximum	40.0	19.0	12.0	7.0	6.0	13.0	28.0
Average	38.860	18.581	11.867	6.373	4.659	12.455	25.530
Std Dev	0.398	0.886	0.563	1.406	1.031	1.324	3.648

Table 3. Tabulated Statistical SNRI Data for Figure 19

Traditional System, Burg Estimator, Symmetric Signal Vectors

SNRI Stats.	Theta 0.000	0.524	1.047	1.571	2.095	2.618	3.142
Maximum	39.0	19.0	13.0	11.0	13.0	19.0	39.0
Average	37.560	17.333	11.493	9.447	11.560	17.665	38.015
Std Dev	3.247	2.019	1.867	1.360	1.583	1.666	1.824

Proposed System, Burg Estimator, Symmetric Signal Vectors

SNRI Stats.	Theta 0.000	0.524	1.047	1.571	2.095	2.618	3.142
Maximum	33.0	12.0	6.0	7.0	12.0	19.0	40.0
Average	31.715	11.046	4.100	6.152	11.445	18.459	39.078
Std Dev	2.319	1.573	1.448	1.537	1.201	1.193	1.288

Table 4. Tabulated Statistical SNRI Data for Figure 20

Traditional System, Burg Estimator, Skew-symmetric Signal Vectors

SNRI Stats.	Theta 0.000	0.524	1.047	1.571	2.095	2.618	3.142
Maximum	39.0	19.0	13.0	11.0	13.0	19.0	39.0
Average	38.004	17.677	11.356	9.387	11.519	17.856	37.627
Std Dev	1.698	1.634	1.890	1.401	1.831	1.770	3.136

Proposed System, Burg Estimator, Skew-symmetric Signal Vectors

SNRI Stats.	Theta 0.000	0.524	1.047	1.571	2.095	2.618	3.142
Maximum	40.0	19.0	12.0	7.0	6.0	13.0	33.0
Average	39.304	18.598	11.587	6.205	4.183	12.221	30.502
Std Dev	1.012	0.995	0.912	1.606	1.301	1.505	4.508

4.0 Bit Error Rate Performance

Up to this point, the performance of both the traditional and the proposed MAMF communication systems has been measured in terms of SNRI. SNRI assists one in determining, on a relative basis, the likelihood of detection and descrimination of signals in noise. The definitive measure of performance in digital communication systems is Bit Error Rate (BER). BER is a statistical measure of the rate at which bit errors occur for a number of bits transmitted. BER is thus more definitive than SNRI since it measures the number of errors and hence the number of successes in communicating a bit stream rather than measuring energy ratios which are related to the probability of detection and discrimination. This chapter investigates the performance of both systems in terms of BER measurements, and makes observations regarding the relationship between BER and SNRI performance measures. BER is dependent upon the ISNR, and so BER as a function of ISNR is computed for both systems. Both systems are designed to communicate binary data in additive narrow-band colored noise conditions. In the first section of this chapter, the systems are described in detail. In the second section, the particular experiments conducted are discussed. In the third section, the results are presented.

4.1 System Descriptions

The general structure of the traditional and proposed MAMF communication systems is the same as discussed previously and depicted in Figure 1 on page 3 and Figure 2 on page 6. The binary data to be communicated is random. The IMSL routine GGNPM is used to generate random numbers with unit variance. If the random number is greater than or equal to zero, then a "1" is chosen as the bit to be communicated; a "0" is chosen otherwise. The signal vectors of both the traditional and proposed systems used to encode the binary data are of length 8 each. The signal vectors of the proposed system are composed of 2 orthogonal basis vectors of equal energy and length 4 each. The energy in the transmitted signal vectors for both systems is equal, and adjusted to obtain the desired ISNR for a particular colored noise. The energy of a transmitted signal vector, E_s, is determined as follows:

$$E_s = ISNR \times R_{ww}(0) \tag{4.1}$$

The signal vector energy is normalized to E_t prior to transmission.

The transmission is simulated by adding colored noise samples to the transmitted signal vectors. The colored noise samples are generated in the same fashion as discussed in Chapter 3 and depicted in Figure 6 on page 41. The colored noise system generates 2032 colored noise samples. Since the colored noise filter which is used to generate the colored noise samples has an infinite impulse response, the first 2000 samples out of the noise coloring filter are discarded to avoid transient affects from influencing the colored noise samples and hence the autocorrelation estimates. The first 2000 noise samples are discarded to minimize the impulse response effects of the IIR digital filter in the colored noise system on the colored noise samples used in the simulation. Of the remaining 32

colored noise samples, the first 16 are used to form the colored noise vector used to estimate the colored noise autocorrelation in both systems. The following 8 are added to the transmitted signal vector of the traditional system, and the last 8 are added to the transmitted signal vector of the proposed system.

In the receiver, the autocorrelation of the colored noise used to form the MAMF's is either the actual or an estimated autocorrelation. The CB estimator discussed in Section 2.2.2 and formulated in equation (2.1), is used to estimate the autocorrelation of the colored noise. The purpose of using the actual autocorrelation is to observe the BER performance of both systems under ideal conditions and is expected to produce the upper limit of BER performance for both systems, as previously done in Chapter 3 for SNRI. The use of the actual colored noise autocorrelation shall furthermore reveal any fundamental relationships between SNRI and BER. The purpose of estimating the colored noise autocorrelation is to observe the performance of both systems in a more practical situation and to note any influence the estimator may have on the BER performance. After the colored noise autocorrelation is determined in the proposed system, the two coefficients which maximize the signal energy out of the i-th MAMF of the proposed system, $c'_{1\,opt\,i}$ and $c'_{2\,opt\,i}$, are determined. The two coefficients for the i-th OSNR maximizer, $c_{1\,i}$ and $c_{2\,i}$, used to determine the optimum coefficients are constrained to maintain constant signal energy as indicated in the development in Section 2.4.1. Since the basis vectors chosen to represent each bit are orthogonal, the coefficients $c_{1\,i}$ and $c_{2\,i}$ are subject to the constraint

$$\sum_{j=1}^{K} c_{j\,i}^2 \;=\; c_{1\,i}^2 + c_{2\,i}^2 \;=\; E_s \tag{4.2}$$

The basis vectors used to represent each bit, the estimated colored noise autocorrelation and the received signal are all processed to detect the i-th bit as follows:

$$\underline{\tilde{s}}_l = \left[\underline{s}_{1\,l} \mid \underline{s}_{2\,l} \right] \begin{bmatrix} c'_{1\,opt\,l} \\ c'_{2\,opt\,l} \end{bmatrix} \tag{4.3}$$

$$R_{v\,l}(l) = E_s R_{ww}(l) + c'_{1\,opt\,l} c'_{2\,opt\,l} \left(R_{ww}(4+l) + R_{ww}(4-l) \right) \tag{4.4}$$

$$\underline{\tilde{I}}_l = \left[\underline{s}_{1\,l} + \underline{n}_1 \mid \underline{s}_{2\,l} + \underline{n}_2 \right] \begin{bmatrix} c'_{1\,opt\,l} \\ c'_{2\,opt\,l} \end{bmatrix} \tag{4.5}$$

The MAMF for each bit in the traditional system is determined from the autocorrelation matrix and the signal vector used to encode the particular bit. The MAMF impulse responses are found as follows:

$$\underline{h}_{0\,TRAD.} = \Phi^{-1} \underline{s}'_0 \tag{4.6}$$

$$\underline{h}_{1\,TRAD.} = \Phi^{-1} \underline{s}'_1 \tag{4.7}$$

where Φ is the Toeplitz autocorrelation matrix formed from either the actual or estimated autocorrelation sequence R_{ww}, and $\underline{s}'_0$, and $\underline{s}'_1$ are the time reversed signal vectors used to encode a "0" and a "1" respectively. The MAMF for each bit in the proposed system is determined from the combined autocorrelation matrix and the signal vector used to encode the particular bit. The MAMF impulse responses are found as follows:

$$\underline{h}_{0\,PROP.} = \Phi_{v0}^{-1} \underline{\tilde{s}}'_0 \tag{4.8}$$

$$\underline{h}_{1\,PROP.} = \Phi_{v1}^{-1} \underline{\tilde{s}}'_1 \tag{4.9}$$

where Φ_v is the autocorrelation matrix formed from the combined actual or estimated autocorrelation sequence, $R_{v\,l}(l)$, as defined in equation (4.4); and $\underline{\tilde{s}}'_0$ and $\underline{\tilde{s}}'_1$ are the time

reversed combined signal vectors, $\bar{s}_0$ and $\bar{s}_1$ respectively. Once the MAMF impulse responses are found, the output of the i-th MAMF, y_{N-1_i}, is determined by convolving the MAMF with the received transmission. The receiver output computation for the proposed system is written in matrix notation as

$$y_{N-1_i} = \mathcal{T}^T h_{i\,TRAD.} \tag{4.10}$$

where $\mathcal{T}$ is the time reversed received transmission composed of the transmitted signal vector with additive colored noise. The receiver output computation for the proposed system is written in matrix notation as

$$y_{N-1_i} = \bar{\mathcal{T}}_i^T h_{i\,PROP.} \tag{4.11}$$

where $\bar{\mathcal{T}}_i$ is the time reversed received transmission of equation (4.5).

Due to the difference in structure between the traditional and proposed MAMF communication systems, the decision rules for determining which bit was most probably transmitted on the basis of y_{N-1} are different for each system. The minimum error probability criterion for a MAMF receiver processing known signal waveforms in additive colored noise developed by Anthony D. Whalen [ADW, p.293] is used in the detector of the traditional MAMF communication system. Given that the probability of transmitting a "1" is equal to the probability of transmitting a "0", i.e. $P(H_1) = P(H_0) = \frac{1}{2}$, the minimum error decision rule selects the hypothesis that a "1" was transmitted, H_1, if

$$2(y_{N-1_1} - y_{N-1_0}) \geq \bar{s}_1^T h_1 - \bar{s}_0^T h_0 \tag{4.12}$$

Two different decision rules are used in the detector of the proposed system. The first decision rule is a simple comparison. The bit associated with the MAMF with the

largest output y_{N-1}, is selected as the bit communicated. For the second decision rule, the output of the MAMF is first normalized with respect to the output of the same MAMF that would be observed if no noise were present prior to making the simple comparison, i.e. the output of the i-th MAMF is first normalized as follows

$$\hat{y}_{N-1_i} = \frac{y_{N-1_i}}{\tilde{s}_i^T h_{i\,PROP.}} \tag{4.13}$$

The bit associated with the MAMF producing the largest normalized output $\hat{y}_{N-1}$, is selected as the bit communicated.

4.2 Experiment Descriptions

Three experiments consisting of two simulations each were conducted. In all of the simulations, 1000 random binary data bits were communicated. The signal vectors used to encode each bit were the same for each system in the first experiment, and likewise for the second experiment. Five different values of ISNR were used in the simulations of the first two experiments. The colored noise used in all of the simulations was narrow-band low-pass colored noise generated by the same colored noise system of Chapter 3 for $\theta = 0$. The colored noise autocorrelation sequence used in the MAMF receiver in each system was either the actual autocorrelation or it was an estimated autocorrelation. The BER performance in each simulation was measured as a function of SNRI. This was done by first computing the SNRI for the particular bit communicated. The bit selected by the detector is compared to the bit communicated to determine whether a bit error occurred. If a bit error occurred, then a bin

corresponding to the integer value of the SNRI was incremented and the type of bit error was recorded. There were two types of bit errors - a "1" detected when a "0" was transmitted, and a "0" detected when a "1" was transmitted. The specific details of each experiment follow.

The signal vectors used in experiment #1 to encode a random binary bit of data, prior to modification to obtain a specific ISNR, are for the traditional system

$$\underline{s}_0 = [\,1\ 0\ 1\ 0\ 0\ 1\ 0\ 1\,]^T \tag{4.14}$$

$$\underline{s}_1 = [\,1\ 0\ 1\ 0\ 0\ -1\ 0\ -1\,]^T \tag{4.15}$$

and for the proposed system

$$\underline{s}_0 = [\,1\ 0\ 0\ 1\ |\ 0\ 1\ 1\ 0\,]^T \tag{4.16}$$

$$\underline{s}_1 = [\,1\ 0\ 0\ -1\ |\ 0\ 1\ -1\ 0\,]^T \tag{4.17}$$

The signal vectors for both the traditional and proposed systems are proportional by a constant to the signal vectors of the traditional and proposed systems in Chapter 3; equations (3.20a) and (3.20b), and equations (3.21a) and (3.21b) respectively. Note from the equations for ISNR and OSNR, (2.26) and (2.29) respectively, and the definition of SNRI that multiplying the signal vector by a constant will not change SNRI. The SNRI for both systems are equal to those computed in Chapter 3 when the colored noise autocorrelation is known. The signal vectors of the traditional system both produce an optimum SNRI of 39.267 dB. The signal vectors for the proposed system, equations (4.16) and (4.17), produce an optimum SNRI of 33.174 dB and 39.815 dB respectively. These signal vectors were chosen to determine if the optimum SNRI influences the BER and/or type of bit error.

The five values of ISNR used in the two simulations of the first experiment were 21.9283, 0.0, -10.0, -20.0, and -30.0 dB. The autocorrelation used to design the MAMF impulse responses for both systems was the actual autocorrelation in the first simulation and it was an estimated autocorrelation in the second simulation. The simulation for which the ISNR is 21.9283 dB and the autocorrelation estimated is identical to comparison 3 cases 1 and 2 of Chapter 3 at $\theta = 0.0$ as depicted in Figure 13 on page 58 and Figure 14 on page 59. The simple comparison scheme is used in the proposed system to determine which bit was probably communicated. The BER performance results for the first experiment are tabulated in Table 5 on page 77 and Table 6 on page 77 respectively.

In experiment #2, the signal vectors used to encode the random binary data, prior to being modified to obtain a specific ISNR, are for the traditional system

$$\underline{s}_0 = [\,1\ 0\ 1\ 0\ 0\ -1\ 0\ -1\,]^T \tag{4.18}$$

$$\underline{s}_1 = [\,-1\ 0\ -1\ 0\ 0\ 1\ 0\ 1\,]^T \tag{4.19}$$

and for the proposed system

$$\underline{s}_0 = [\,1\ 0\ 0\ -1\ |\ 0\ 1\ -1\ 0\,]^T \tag{4.20}$$

$$\underline{s}_1 = [\,-1\ 0\ 0\ 1\ |\ 0\ -1\ 1\ 0\,]^T \tag{4.21}$$

These signal vectors are chosen since they produce an optimum SNRI of 39.267 dB for the traditional system and 39.815 dB for the proposed system. The SNRI of the two systems is approximately equal, so that the direct performance comparison of both systems is fair. Note that the relationship between $\underline{s}_0$ and $\underline{s}_1$ is

$$\underline{s}_0 = -\underline{s}_1 \tag{4.22}$$

This relationship produces the *optimum or ideal binary communication system* [ADW, p. 163]. The resulting binary communication system is *ideal* because the probability of error is minimal. The probability of error is minimal when the time crosscorrelation coefficient for the signal vectors is -1 which is true only if equation (4.22) is satisfied.

The five values of ISNR used in the two simulations of the second experiment were 0.0, -10.0, -20.0, -30.0, and -35.0 dB. The autocorrelation used to design the MAMF impulse responses for both systems was the actual autocorrelation in the first simulation and it was an estimated autocorrelation in the second simulation. The simple comparison scheme is used in the proposed system to determine which bit was probably communicated. The BER performance results for the two simulations of the second experiment are tabulated in Table 7 on page 78 and Table 8 on page 78 respectively.

The purpose of experiment #3 is to investigate the BER performance of the proposed system with a detector that first normalizes the output prior to the simple comparison. In the first simulation of this experiment, the signal vectors are the same as those used in experiment #1. The signal vectors in the second simulation are the same as those in experiment #2. Only one ISNR is thus used in each simulation, and it is chosen to be -30 dB to contrast the BER performance under an adverse condition. The BER performance results for the two simulations are tabulated in Table 9 on page 79 and Table 10 on page 79 respectively.

4.3 Experimental BER Results

The following tables are the results of the aforementioned experiments.

Table 5. Experiment #1, Simulation 1, Bit Errors / 1000 Bits vs ISNR

Autocorrelation Known

System	Bit	Signal Vector	ISNR (dB) 21.93	0	-10	-20	-30
Trad.	0	1 0 1 0 0 1 0 1	0	0	0	0	15
	1	1 0 1 0 0 -1 0 -1	0	0	0	0	7
Prop.	0	1 0 0 1 0 1 1 0	0	0	0	14	153
	1	1 0 0 -1 0 1 -1 0	0	0	0	0	2

Table 6. Experiment #1, Simulation 2, Bit Errors / 1000 Bits vs ISNR

Autocorrelation Estimated, CB Estimator w/ 16 Samples

System	Bit	Signal Vector	ISNR (dB) 21.93	0	-10	-20	-30
Trad.	0	1 0 1 0 0 1 0 1	0	0	1	44	185
	1	1 0 1 0 0 -1 0 -1	0	0	2	53	151
Prop.	0	1 0 0 1 0 1 1 0	0	0	0	22	152
	1	1 0 0 -1 0 1 -1 0	0	0	0	2	77

Table 7. Experiment #2, Simulation 1, Bit Errors / 1000 Bits vs ISNR

Autocorrelation Known

System	Bit	Signal Vector	ISNR (dB) 0	-10	-20	-30	-35
Trad.	0	1 0 1 0 0 -1 0 -1	0	0	0	0	32
	1	-1 0 -1 0 0 1 0 1	0	0	0	0	17
Prop.	0	1 0 0 -1 0 1 -1 0	0	0	0	1	21
	1	-1 0 0 1 0 -1 1 0	0	0	0	0	20

Table 8. Experiment #2, Simulation 2, Bit Errors / 1000 Bits vs ISNR

Autocorrelation Estimated, CB Estimator w/ 16 Samples

System	Bit	Signal Vector	ISNR (dB) 0	-10	-20	-30	-35
Trad.	0	1 0 1 0 0 -1 0 -1	0	0	1	76	145
	1	-1 0 -1 0 0 1 0 1	0	0	1	67	126
Prop.	0	1 0 0 -1 0 1 -1 0	0	0	0	0	35
	1	-1 0 0 1 0 -1 1 0	0	0	0	3	32

Table 9. Experiment #3, Simulation 1, Bit Errors / 1000 Bits

ISNR = -30 dB

System	Bit	Signal Vector	Autocorrelation Actual	Autocorrelation Estimated
Trad.	0	1 0 1 0 0 1 0 1	15	185
	1	1 0 1 0 0 -1 0 -1	7	151
Prop.	0	1 0 0 1 0 1 1 0	274	246
	1	1 0 0 -1 0 1 -1 0	233	240

Table 10. Experiment #3, Simulation 2, Bit Errors / 1000 Bits

ISNR = -30 dB

System	Bit	Signal Vector	Autocorrelation Actual	Autocorrelation Estimated
Trad.	0	1 0 1 0 0 -1 0 -1	0	76
	1	-1 0 -1 0 0 1 0 1	0	67
Prop.	0	1 0 0 -1 0 1 -1 0	0	0
	1	-1 0 0 1 0 -1 1 0	480	480

5.0 Summary and Conclusions

The results of the comparison which contrasts the maximum attainable SNRI for both the traditional and proposed MAMF communication systems is given in Figure 8 on page 53. The results indicate that the absolute maximum attainable SNRI for the traditional MAMF communication system simulated herein is greater than the absolute maximum attainable SNRI for the proposed MAMF communication system at all of the discrete colored noise center frequency points. The absolute maximum SNRI for the tradtional system is not always greater than the absolute maximum SNRI for the proposed system since the maximum SNRI is determined by the minimum eigenvalue of the real symmetric Toeplitz colored noise autocorrelation matrix. These results must be kept in mind when considering the other comparisons.

The results of the comparison which contrasts the performance of both systems when the colored noise autocorrelation is known rather than estimated are given in Figure 9 on page 54, Figure 10 on page 55, Figure 11 on page 56, and Figure 12 on page 57. From Figure 9 on page 54 and Figure 10 on page 55, wherein the traditional system is optimized to produce its maximum SNRI for the colored noise center frequency $\theta = 0.0$, the performance of the traditional system is better than that of the

proposed system in the vicinity of the point of optimization, as expected from the results of the earlier comparison. Note however that the SNRI of the traditional system is less than 0 dB, i.e. the MAMF degrades the performance of the system, when the color of the noise is very different from the noise color for which it was optimized. The SNRI for the proposed system is never less than 0 dB and hence always actually improves the performance of the system. The orthonormal basis vectors chosen for the proposed system were not optimized to produce its maximum SNRI. From Figure 11 on page 56 and Figure 12 on page 57, wherein the traditional system is optimized to produce its maximum SNRI for the colored noise center frequency $\theta = 0.5\,\pi$, the performance of the traditional system is never less than 0 dB and hence the traditional MAMF receiver does not degrade the performance of the system. The SNRI of the traditional system is greater than the SNRI of the proposed system for $\theta = 0.5\,\pi$; however, the SNRI of the traditional system is not greater than SNRI of the proposed system over all the discrete colored noise center frequencies. From Figure 12 on page 57, wherein the orthonormal basis vectors of the proposed system are skew-symmetric, the colored noise need not deviate very far from the point for which the traditional system was optimized for the SNRI of the proposed system to exceed the SNRI of the traditional system. This is quite significant when one considers that the maximum attainable SNRI for the traditional system is greater than that of the proposed system. The results of this comparison indicate that the proposed system can be designed to be robust with respect to time-varying noise color and outperform the traditional system as the color of the noise varies.

The comparison in which the performance of both systems is contrasted when the colored noise autocorrelation is known and the traditional system is not optimized for any particular noise color are given in Figure 13 on page 58, Figure 14 on page 59, Figure 15 on page 60, and Figure 16 on page 61. From Figure 13 on page 58 and

Figure 14 on page 59, wherein the signal vector for the traditional system is symmetric and skew-symmetric respectively, the traditional system can be made robust for the time-varying narrow-band colored noise used therein by not optimizing the system for any particular noise color. Note however, that the SNRI of the proposed system can again exceed the SNRI of the traditional system. From Figure 15 on page 60 and Figure 16 on page 61, wherein the transmitted signal vector for the traditional system is the concatenation of the orthonormal basis vectors for the proposed system, i.e. the transmitted signal vectors for both systems were identical. The purpose of making the transmitted signal vector for both systems identical is to investigate the performance for a receiver composed of both the traditional and proposed receivers. The results of the last two cases indicate that such a system could produce a high SNRI by selecting the receiver that has the greatest signal energy at the output of the MAMF(s) and be robust to time-varying noise color.

The results of the comparison which contrasts the performance of both systems when the colored noise autocorrelation is estimated and the traditional system is not optimized for any particular noise color are illustrated in Figure 17 on page 62, Figure 18 on page 63, Figure 19 on page 64, and Figure 20 on page 65, and tabulated in Table 1 on page 66 and Table 2 on page 66. The colored noise autocorrelation is estimated by the classical biased estimator in Figure 17 on page 62 and Figure 18 on page 63. The colored noise autocorrelation is estimated by the Burg estimator in Figure 19 on page 64 and Figure 20 on page 65. When the autocorrelation is known, OSNR is optimum as defined in equation (2.35) and hence SNRI is optimum too. The signal vectors for both systems are identical to those used in Figure 13 on page 58 and Figure 14 on page 59, thus the optimum SNRI for the cases of this comparison are given in Figure 13 on page 58 and Figure 14 on page 59. In all four cases of this comparison, the maximum SNRI attained for both systems is equal to the optimum

SNRI. This is of particular importance for the proposed system since it indicates that when the signal energy at the output of the MAMF is maximized, SNRI can attain its optimum value. Note that at some points where the optimum SNRI of the traditional system is greater than that of the proposed system, the average SNRI of the proposed system is greater than that of the traditional system. From Table 1 on page 66 and Table 2 on page 66, the SNRI standard deviation for the proposed system is less than the SNRI standard deviation for the traditional system at most of the colored noise points. This is of particular importance since it again indicates the robust nature of the proposed system. Since the proposed system optimizes the OSNR with respect to the estimated noise, the proposed system is able to yield a high average SNRI with a small SNRI standard deviation. Note furthermore that if the optimum SNRI is close to 0 dB, then the SNRI attained from either system can be less than 0 dB due to the stochastic nature of the SNRI when the colored noise autocorrelation is estimated. The proposed system can thus outperform the traditional system when the noise autocorrelation is estimated even when the optimum SRNI of the traditional system is greater than the optimum SNRI of the proposed system due to its robust nature.

In summary of the results of Chapter 3, it was observed that the performance of the MAMF receiver optimized for a particular noise color can degrade the overall performance of the communication system as the color of the noise varies; however, the performance of the MAMF receiver in the proposed system did not degrade the overall performance of the communication system. The proposed MAMF communication system is thus more robust to time-varying noise color than the traditional system optimized for a particular noise color. Due to the robust nature of the proposed system, the performance of the proposed system can exceed the performance of the traditional system even when the absolute maximum performance for the traditional system is greater than the absolute maximum performance for the proposed system. When the

traditional system is not intentionaly maximized for a particular noise color, its performance can become robust to time-varying noise color; however, the performance of the traditional system can be less than that of the proposed system. By combining the receivers of both the traditional and proposed communication systems and transmitting the signal vector used in the proposed system, the resulting system would be robust to time-varying noise and could use the receiver with the greatest SNRI. In conclusion, the proposed system is robust to time-varying noise color and thus can outperform the traditional system when the color of the noise varies.

The first experiment of Chapter 4 was conducted to determine if a substantial difference in the optimum SNRI of two moving-average matched filters used to detect two different bits of data would influence BER performance. The maximum SNRI for the traditional system are equal, while for the proposed system, the maximum SNRI for the MAMF used to detect a "0" is 6.741 dB less than the MAMF used to detect a "1." From Table 5 on page 77 wherein the actual colored noise autocorrelation was used, 14 bit errors were detected for the proposed system at -20 dB ISNR while none were detected for the traditional system; furthermore, 155 bit errors were detected for the proposed system at -30 dB ISNR while only 22 were detected for the traditional system. Of the 155 bit errors at -30 dB ISNR in the proposed system, 153 occurred when a "0" was transmitted and a "1" was detected and 2 occurred when a "1" was transmitted and "0" was detected. From the distribution of errors at -30 dB ISNR, it is evident that the difference in optimum SNRI between the two moving-average matched filters used to detect each bit has a significant effect on the BER performance. This is intuitively substantiated when one considers how a MAMF receiver functions. From Chapter 2, a MAMF is designed to maximize OSNR. As the ISNR decreases, the OSNR decreases. The ISNR can reach a point such that the OSNR produced by the MAMF is less than unity thus decreasing the probability of detection. If the optimum SNRI of one MAMF

is less than the optimum SNRI of another MAMF, the MAMF with the smaller optimum SNRI will produce an OSNR less than unity before the MAMF with the greater optimum SNRI as the ISNR decreases. The 6.741 dB difference in optimum SNRI between the moving-average matched filters of the proposed system is the cause of the imbalance in the type of bit errors observed.

From Table 6 on page 77 wherein the colored noise autocorrelation was estimated, the imbalance in the type of bit errors for the proposed system still remains; however, the imbalance is not as great as in the first simulation. This is due to the stochastic nature of the SNRI. When the autocorrelation of the colored noise is estimated, the SNRI of a MAMF communication system is a stochastic process. The SNRI of the MAMF used to detect a "0" could be greater than or equal to the SNRI of the MAMF used to detect a "1", hence the output of the MAMF used to detect a "0" would be more likely to be greater than the output of the MAMF used to detect a "1". The imbalance in the errors is thus not expected to be as great as the imbalance observed in the first simulation. The number of errors in the traditional system increased considerably compared to the number of errors observed in the first simulation. From Table 1 on page 66 and Table 2 on page 66, the average SNRI for the traditional system is less than that for the proposed system; furthermore, the SNRI standard deviation for the traditional system is larger than that for the proposed system. The statistical SNRI performance of the traditional system is thus not as good as the statistical SNRI performance of the proposed system. The difference in the statistical SNRI performance between the two systems is the cause for the difference in their respective BER performances.

Experiment #2 of Chapter 4 was conducted to compare the performance of the traditional optimum binary MAMF communication system with the proposed optimum binary MAMF communication system. From Chapter 3, the SNRI of the traditional

system was 39.266 dB, and the SNRI of the proposed system was 39.814 dB. The SNRI performance of both systems is thus approximately the same. From the results in Table 7 on page 78, wherein the actual colored noise autocorrelation was used, the first bit error occurred at -30 dB ISNR in the proposed system. At -35 dB ISNR, the number of errors was greater for the traditional system than the number of errors for the proposed system. From the results in Table 8 on page 78, wherein the colored noise autocorrelation sequence was estimated, the first bit errors occurred at -20 dB ISNR in the traditional system. The number of bit errors at -30 and -35 dB ISNR for the tradional system is substantially larger than the number of bit errors for the proposed system. The difference in bit errors is due to the statistical SNRI characteristics of the traditional system not being as good as those of the proposed system as previously mentioned. Note that the number of errors observed for the proposed system is approximately equally divided over the two possible types. This balance is due to the equal optimum SNRI and equal statistical SNRI characteristics of each MAMF.

Experiment #3 of Chapter 4 was conducted to determine the performance of the detector used in the proposed system which first normalizes the output of each filter prior to conducting a simple comparison to determine which bit was most probably communicated. From the results in Table 9 on page 79, the numbers for each type of bit error were more balanced than in the first experiment; however, the total number of each type of bit error was substantially increased. From the results in Table 10 on page 79, a larger number of errors occurred when a "1" was detected whereas a "0" was transmitted; furthermore, the number of bit errors has increased substantially. The proposed detector thus balances the number of each type of error when the colored noise autocorrelation is known at the cost of an enormous increase in the total number of bit errors. The detector performs poorly compared to the detector used in the first two

experiments, when the colored noise autocorrelation is estimated and the signal vectors are chosen such that the communication system is optimum.

In summary of the results of Chapter 4, it is important to either insure that the optimum SNRI and statistical SNRI characteristics of each MAMF in the receiver are approximately the same or to compensate for the difference in the receiver. Care must be taken when selecting the detector to compensate for differences in SNRI due to possible impacts if the conditions under which the system is operating change. SNRI is a good indicator of BER performance when the ISNR is specified. It is possible for the proposed system to substantially outperform the traditional system. This is possible even when the optimum SNRI of the proposed system is less than that of the traditional system due to the statistical characteristics of the SNRI when the colored noise autocorrelation is estimated.

In closing, a new MAMF communication system was proposed herein. The proposed system has many promising features. The foremost advantageous feature of the proposed system is that it is robust to time-varying colored noise. The SNRI and BER performance of the proposed system can exceed that of the traditional MAMF communication system even when the traditional system is optimized. Only narrow-band colored noise was used in the simulations, thus the performance of the proposed system under different colored noise still remains to be investigated. Both the detection scheme of the MAMF receiver in the proposed system used herein and the choice of signal vectors also require further investigation.

BIBLIOGRAPHY

[ACB] A. Cantoni and P. Butler, "Properties of the eigenvectors of per-symmetric matrices with applications to communication theory," IEEE Trans. Commun., vol. COM-24, pp. 804-809, Aug. 1976.

[ADW] A. D. Whalen, Detection of Signals in Noise, Academic Press Inc., C 1971.

[APB] A. Cantoni and P. Butler, "Eigenvalues and eigenvectors of symmetric centrosymmetric matrices," Linear Algebra and Its Applications, vol. 13, pp. 275-288, 1976.

[BCB] K.A. Becker and A.A. Beex, "The Effects of Spectral Estimation on Matched Filter Design," 27th Midwest Symposium on Circuits and Systems, June 11-12, 1984, Morgantown, VW, pp. 211-214.

[BEB] A.A. Beex and K.A. Becker, "Spectral Estimation and Matched Filter Performance," IEEE International Conference on Acoustics, Speech, and

Signal Processing (ICASSP '84), March 19-21, San Diego, CA, pp.31.4.1-4.

[CTC] C. Chen, Introduction to Linear System Theory, New York: Holt, Rinehart and Winston, 1970, pp.409.

[DBS] J.P. Dugre, A.A. Beex, and L.L. Scharf, "Generating covariance sequences and the calculation of quantization and rounding error variances in digital filters," IEEE Transactions on Acoustics, Speech, and Signal Processing, vol. ASSP-28, pp. 102-104, Feb. 1980.

[JAC] J.A. Cadzow, "Generalized Digital Matched Filtering," 12th Annual Southeastern Symposium on System Theory, Virginia Beach, VA, May 19-20, 1980, pp. 307-312.

[JMK] John Makhoul, "On the Eigenvectors of Symmetric Toeplitz Matrices," IEEE Transactions on Acoustics, Speech, and Signal Processing, Vol. ASSP-29, No. 4, August 1981, pp 868-872.

[KAB] K.A. Becker, "Effects of Spectral Estimation on Matched Filter Design," M.S. Thesis, Virginia Polytechnic Institute and State University, May, 1985.

[MBT] A.B. Martinez and J.B. Thomas, "Finite Length Discrete Matched Filters," Nineteenth Annual Allerton Conference on Communication, Control, and Computing, Sept. 30 - Oct. 2, 1981.

[PAP] A. Papoulis, Probability, Random Variables and Stochastic Processes, McGraw-Hill Book Company, New York, 1984.

[WLB] William L. Brogan, Modern Control Theory, Prentice-Hall Inc., New Jersey, 1985.

The vita has been removed from the scanned document